IEEE Access
Multidisciplinary | Rapid Review | Open Access Journal

Received 10 January 2024, accepted 18 January 2024, date of publication 24 January 2024, date of current version 15 February 2024.

Digital Object Identifier 10.1109/ACCESS.2024.3358280

TOPICAL REVIEW

Low Frequency Multi-Robot Networking

BRIAN M. SADLER[1], (Life Fellow, IEEE), FIKADU T. DAGEFU[1], (Senior Member, IEEE), JEFFREY N. TWIGG[1], (Member, IEEE), GUNJAN VERMA[1], PREDRAG SPASOJEVIC[2], (Senior Member, IEEE), RICHARD J. KOZICK[3], (Senior Member, IEEE), AND JUSTIN KONG[1], (Senior Member, IEEE)

[1]DEVCOM Army Research Laboratory, Adelphi, MD 20783, USA
[2]Department of Electrical and Computer Engineering, Rutgers University, Piscataway, NJ 08854, USA
[3]Department of Electrical and Computer Engineering, Bucknell University, Lewisburg, PA 17837, USA

Corresponding author: Brian M. Sadler (brian.sadler@ieee.org)

ABSTRACT Autonomous teams of unmanned ground and air vehicles rely on networking and distributed processing to collaborate as they jointly localize, explore, map, and learn in sometimes difficult and adverse conditions. Co-designed intelligent wireless networks are needed for these autonomous mobile agents for applications including disaster response, logistics and transportation, supplementing cellular networks, and agricultural and environmental monitoring. In this paper we describe recent progress on wireless networking and distributed processing for autonomous systems using a low frequency portion of the electromagnetic spectrum, here defined as roughly 25 to 100 MHz with corresponding wavelengths of 3 to 12 meters. This research is motivated by the desire to support autonomous systems operating in dense and cluttered environments by harnessing low frequency propagation, where meters long wavelengths yield significantly reduced scattering and enhanced penetration of obstacles and structures. This differs considerably from higher frequency propagation, requiring different low frequency propagation models than those widely employed for other bands. Progress in use of low frequency for autonomous systems has resulted from combined advances in low frequency propagation modeling, networking, antennas and electromagnetics, geolocation, multi-antenna array distributed beamforming, and mobile collaborative processing. This article describes the breadth and the depth of interaction between areas, leading to new tools and methods, especially in physically complex indoor/outdoor, dense urban, and other challenging scenarios. We bring together key results, models, measurements, and experiments that describe the state of the art for new uses of low frequency spectrum for multi-agent autonomy.

INDEX TERMS Low frequency spectrum, low frequency propagation, autonomy, multi-robot networking, complex environments, geolocation, distributed beamforming, parasitic arrays, cognitive radio.

I. INTRODUCTION

Global advances in autonomous unmanned ground and air vehicles (UGVs, UAVs), driverless cars, and other collaborative intelligent systems are reliant on communications networking and distributed processing. Consequently, cognitive wireless networks are needed for these autonomous mobile agents as they are developed and applied for disaster response, logistics and transportation, supplementing cellular networks, agricultural sensing, environmental monitoring, security and military operations, and other areas.

In this paper we describe recent progress on wireless networking and distributed processing for autonomous systems, using a low frequency portion of the electromagnetic spectrum. We define *low frequency* as roughly 25 to 100 MHz, with corresponding wavelengths of 3 to 12 meters. This occupies the upper portion of the High Frequency (HF) and the lower portion of the Very High Frequency (VHF) spectrum bands. The study of low frequency for autonomy is motivated by the desire to support autonomous systems operating in dense and cluttered environments by harnessing

The associate editor coordinating the review of this manuscript and approving it for publication was Walid Al-Hussaibi.

low frequency radio signal propagation, where the meters long wavelengths result in significantly reduced scattering and enhanced penetration of obstacles and structures.

Progress in use of low frequency for autonomous systems has resulted from combined advances in communications, networking, antennas and electromagnetics, multi-antenna array beamforming, and mobile distributed collaborative processing. The coupling of networking and autonomy, taking full advantage of the low frequency signal propagation characteristics, is leading to new tools and methods for effective mobile autonomous teams.

To provide review and perspective we:

- Summarize multi-robot networking challenges and state of the art in complex environments
- Survey and summarize low frequency usage and propagation modeling for mobile communications
- Review advances in low frequency technology including antennas, processing, and networking with a focus on multi-agent autonomy
- Review spatial and array processing at low frequency
- Offer perspective on challenges and opportunities for exploiting low frequency in multi-agent autonomous systems in difficult conditions with uncertain networks

A. OUTLINE

Section II describes the many challenges and state of the art in autonomous multi-robot networking, including network topology and mobility, propagation mapping, distributed processing and control, and mobile ad hoc networking. Section III looks at low frequency spectrum allocation and use cases. Low frequency propagation studies and modeling are described in Section IV, including the variety of effects and models for complex environments, and then summarizes the state of the art in low frequency propagation modeling. Section V reports recent short range low frequency communications studies, chiefly for highly cluttered indoor/outdoor environments, with an eye towards applicability to UAVs and UGVs. Studies include indoor/outdoor software defined radio experiments and channel characterization, and comparisons between lower and higher frequency usage.

Section VI provides a brief discussion of key ideas and recent progress in low frequency antennas, especially miniature sub-wavelength designs. Electrically small antennas are a critical enabling technology for compact mobile platforms to efficiently use low frequencies.

Section VII describes recent progress in geolocation, including phase-based and receive signal strength (RSS) based methods. These are closely linked with propagation modeling. RSS-based methods have been developed for autonomous mobile agents, such that a single mobile agent can collect RSS measurements and infer source direction.

Section VIII considers low frequency distributed beamforming where multiple agents collaborate to form an antenna array. The use of low frequency relaxes localization and synchronization requirements, and collaborative beamforming algorithms have been developed for autonomous teams.

Section IX describes unique low frequency arrays that exploit parasitic electromagnetic coupling between antenna elements for enhanced directionality. This approach has been devised for ultra-miniature arrays that can be deployed on a single small platform, and multi-agent configurations where autonomous platforms spatially align themselves into an array.

Sections X and XI focus on recent advances in low frequency ad-hoc networking for mobile agents. Section X describes progress on multi-user coding techniques that are effective in quasi-synchronous low frequency channels, and Section XI details non-orthogonal multi-agent access schemes.

Finally, Section XII provides a discussion of open research questions, challenges, and opportunities for enhancing and combining low frequency technology for collaborative autonomous systems.

II. MULTI-ROBOT NETWORKING: CHALLENGES AND STATE OF THE ART

Developing and deploying collaborative multi-agent autonomous systems brings many challenges including ad-hoc network topology tracking and management, indoor/outdoor operations, sensing and situational awareness, UAV-UGV collaboration, distributed control, and human-machine integration. Autonomous teams are expected to self- and jointly localize, map and explore, collaboratively learn, and adaptively network in difficult and adverse conditions. Sophisticated collaborative behaviors require joint perception and information sharing, dynamic planning and tasking, and human interaction.

Multi-robot autonomous systems generally rely on wireless networking to support collaboration, and can benefit from advances in cognitive networking. The combination and rich interplay between wireless networking and autonomy benefits both areas. Collaborative autonomy requires networking, and wireless networking can be enhanced by incorporating mobile autonomous agents into the network, e.g., using intelligent mobile relays.

Ensuring wireless communications network reliability among autonomous agents is very challenging in complex environments due to increased propagation channel complexity caused by the various wave propagation mechanisms including reflection, diffraction, multiple scattering, and surface waves in the case of near-ground antennas. The dominant propagation mechanisms can vary dramatically with the wavelength and the environmental complexity including size, density and dielectric properties of scatterers and structures that are present.

A key factor governing propagation is the relative size of the wavelength λ compared to the size d of reflectors in the environment. Generally, scattering dominates when $\lambda \ll d$, whereas scattering is significantly reduced when $\lambda \gg d$. For example, as the signal frequency increases above 1 GHz and the wavelength decreases to centimeters then reflection and refraction tend to dominate in urban scenes. The resulting

multipath propagation induces signal fading with highly varying signal strength across space and time, and this greatly complicates mobile wireless networking solutions. In contrast, low frequencies with meters long wavelengths have reduced scattering and better penetrate obstacles and structures.

The study of low frequency methods is motivated by the difficulty of maintaining links in complex scenes, and the desire for persistent low bandwidth connectivity that is less susceptible to fading. The low frequency propagation can be harnessed in various ways to support multi-robot systems, as described in this article.

A. MULTI-ROBOT NETWORKING

The need for a systems-based approach for multi-robot networking has long been recognized [1]. The multi-robot network problem includes physical layer, medium access control (MAC), routing, and geometric connectivity topology, all in the context of the autonomous system goals. Adversarial electromagnetic environments make the multi-robot coordination challenging in many ways [2]. A recent review of multi-robot collaboration and networking reveals the challenges and issues that arise due to a lack of co-design and co-optimization of robots and the networks they employ [3]. As the state of the art in multi-agent collaboration progresses to include more sophisticated behaviors over longer time and spatial scales there is a corresponding need to make them resilient to rapid disruptive changes in the environment, changes in the networking topology, agent failures, and other forms of unanticipated and unpredictable change [4].

B. NETWORK TOPOLOGY AND AGENT MOBILITY

Highly uncertain and variable communications connectivity is a major challenge for multi-robot systems relying on ad hoc networks, such as in disaster relief scenarios where a cellular wireless infrastructure may not be available [5]. Operating with commonly available radios in the UHF radio band (300 MHz to 3 GHz) results in multipath fading and received signal strength that is highly fluctuating over short spatial scales when operating in dense and cluttered environments (see Section IV).

Addressing these challenges, a hybrid systems architecture was proposed that enables a multi-robot team to complete a task in a complex fading environment, self-organizing into a multihop ad hoc network [6]. This joint control strategy maintains connectivity through a group of robots as a task progresses. A joint optimization framework for mobile wireless infrastructure on demand is developed in [7]. This method alternates between finding optimal network routes to support data flows between agents and improving the performance of the network by repositioning a collection of mobile relay nodes. Joint designs can significantly reduce inefficiencies due to agents moving to areas of poor connectivity, as easily happens with UHF radios in complex indoor/outdoor environments. Agents dynamically coordinate movement to ensure information is communicated between specific agents at the appropriate time and space.

The forms of collaboration and information sharing between agents can be organized in various ways. A three-tier organization consisting of connectivity, communication, and action graphs was proposed as a general model, and their interaction was studied [8]. Different functions among these three graphs leads to different desired topologies that, if achieved, enhance the ability of the agents to achieve their objectives.

The desired network topology is linked to the particular multi-robot task scenario. Finding the appropriate topology can often be cast as an optimization problem, although the solution may be complex and new solutions may be needed as the task progresses. A learning-based approach has been developed using a convolutional neural network (CNN) to find an optimal topology based on the collaborative task [9]. This approach offers generalization over a number of different tasks, and scales with the number of agents. When the CNN is trained with a sufficient number of agents then inference can be carried out with a larger number of agents. An additional benefit of this approach is that the CNN has fixed computational complexity, whereas the complexity of the original optimization problem will typically scale with the size of the graph.

Many studies have considered integrating UAVs into cellular systems [10]. This includes incorporating a UAV as a mobile basestation to dynamically extend and enhance the cellular system, as well as developing protocols and methods for serving UAVs from a basestation. Robots can also be used to provide a relay between a mobile user and a basestation, e.g., by autonomously moving the relay to minimize energy usage [11], or linking two robot groups [12].

The development of mmWave arrays and optical communications for mobile devices is driving new research focus on line-of-sight (LoS) links [13]. Agents employing these can use mobility to establish LoS, e.g., using opportunistic or pre-planned rendezvous to achieve mutual visibility. This can be extended to multi-agent control to achieve a placement where each agent is connected to all others through a sequence of visibility pairings, thus guaranteeing that LoS communications is sufficient to network among all agents [14].

C. MOBILE AD HOC ROBOTIC NETWORKS

Aside from the autonomous agent perspective, the mobile ad hoc network (MANET) problem is difficult in general and can require significant networking overhead to maintain at least one or two hop connectivity, especially in complex environments [15]. Alternatives to finding and maintaining a particular network topology include oportunistic and scheduled communications.

Opportunistic methods typically assume that agents will have connectivity randomly but within some time scale.

When agents have geolocation information, as is common in robotics, then position-based opportunistic routing can be employed [16]. Opportunistic routing protocols can support dynamic mobile ad-hoc networks [17], and side information such as residual energy and link quality can be incorporated into local routing decisions [18]. Opportunistic ad hoc networking can also apply dynamic spectrum access techniques to transmit on open channels as needed [19], e.g., using a sense and then transmit scheme [20].

Scheduled communications can be achieved through mobile rendezvous, such as forming periodic communication links within or across robot groups, using a prescribed time-varying topology [21].

Agents may also react to changing channel conditions and move in a way that enhances connectivity, without explicit topology control. For example, mobile agent pairs can monitor their respective received signal strength as they move, and adjust their positions to maintain good connectivity [22]. This could be extended to link with an overall collaborative objective, such as a leader-follower scenario [23].

MANETs support many applications that connect human users, and might not have any autonomous nodes. So, it is useful to recognize that autonomous agents can be deployed in such cases solely to augment and support MANETs. As demonstrated in the works described above, when coupled with controlled mobility a multi-robot system can adjust positioning, incorporate mobile autonomous relays, and adapt the networking protocol to handle nonstationarity and stochastic connectivity in order to support a MANET, as well as to carry out a desired distributed computation or execute collaborative control.

The collection of methods noted above offer a variety of tools for network topology control, from opportunistic to fully planned, and reactive as needed. These methods can be combined into hybrids, and/or dynamically switched depending on the operating context.

D. RADIO PROPAGATION MAPPING

Autonomous agents can be deployed to map the radio propagation in a complex environment. The resulting radio-map can be combined with a geometric map to enable multi-robot mobility planning and task execution. When UHF radios such as cellular and WiFi are employed, as is typical in the literature, then multi-robot methods must adapt to fading environments where signal strength and communications channels have high spatial and temporal variability.

Autonomous agents can collaborate and map out connectivity regions [24]. Gaussian process models have been developed as part of a strategy to map robot connectivity and enable robust multi-robot deployment that adapts to local communications conditions while carrying out a group task [25]. Also, a method for finding the connectivity region around a basestation (a boundary inside which the received signal strength is above a threshold) has been developed [26]. This method uses the received signal strength spatial gradient to efficiently find and follow the connectivity boundary around the basestation and sketch it in a map.

E. DISTRIBUTED PROCESSING AND CONTROL

Collaborative multi-robot control, distributed processing, and learning are often cast with a nearest-neighbor communications model, and algorithms iterate between local communication exchanges and per-agent computation, e.g., see Bullo [27]. This includes many well known consensus and distributed algorithms. Distributed optimization is an important and general form of multi-agent collaboration and learning, with many tradeoffs in computation and communications [28].

Many nearest-neighbor distributed algorithms have relatively low communications payload per transmission, such as in consensus algorithms [29]. Consensus methods can be tuned in various ways to limit the number of exchanges needed. For example, consensus can be enforced within a local subset of agents without requiring agents far away to agree, and consensus can be relaxed from equality to a bounded inequality constraint [30]. Nevertheless, distributed consensus-type algorithms require persistent local connectivity for convergence or to maintain stable distributed multi-robot control (at least at the average topology level).

Multi-agent control studies verify the need for persistent connectivity in the class of nearest-neighbor algorithms. A study of flocking and network interaction, where the network links (the graph edges) change randomly, showed that regardless of switching, flocking convergence to a common velocity vector and stabilization of inter-agent distances is guaranteed as long as the network remains connected at all times [31]. Generally, the network topology needs some form of persistent connectivity, although individual links may appear and disappear randomly, e.g., see [32]. Careful consideration for maintaining the desired network topology among robots is important to satisfy multi-robot control objectives and stability when using nearest-neighbor methods [33].

Recently proposed graph neural network (GNN) methods for learning distributed controllers are similarly based on local neighbor information exchange, and show good robustness to random topology variation [34], [35], [36]. The learned agent controllers can be scaled to large numbers of agents, are tolerant to agent dropouts and new agent additions, and are robust to communication dropouts.

Partially observable Markov decision processes (POMDPs) are a key tool in robotics, and these have been extended to the multi-robot case using decentralized coordination (referred to as Dec-POMDP); e.g., see the recent survey [37]. These methods provide for a range of coordination options, from agreeing on a joint policy beforehand such that agents do not explicitly communicate, to utilizing consensus algorithms during task execution through nearest-neighbor communications.

III. LOW FREQUENCY AND SPECTRUM USAGE

In the US and Canada, and similarly around the world, the lower portion of the VHF band is partitioned into many categories and applications including land mobile, military, amateur radio, radio astronomy, and television and FM radio broadcast [38], [39], [40].

Public safety networking (PSN) is evolving from traditional land mobile radio (LMR) operating in portions of VHF and UHF, to incorporate and interoperate with cellular LTE technology, and internetworking between LMR and emerging LTE technology will provide extensive new PSN services [41], [42], [43]. LTE-based infrastructure has the potential to provide new and advanced PSN capability [44], and robust low-latency push to talk is an important aspect [45]. The combination of cellular and mobile ad hoc networks (MANETs) for disaster and emergency scenarios is also of significant interest, e.g., see [46].

Classic studies of land mobile radio, such as Parson's comprehensive book [47], provide broad background on propagation measurements and modeling, and communications engineering. Mobile radio in VHF and microwave bands resulted in many studies of an elevated base station and near-earth mobile, typically with medium to high power transmission (Watts to kW) at ranges of 1 km and beyond, and were often motivated to provide coverage prediction and identification of blackout areas. Many VHF and microwave studies rely on asymptotic approximation of Maxwell's equations as the frequency goes to infinity, with a resulting assumption that the wavelength is much less than the size of objects encountered in the environment [48]. This leads to ray theory (geometrical optics, geometric theory of diffraction) for approximating propagation. The focus on longer range and upper VHF to UHF and higher frequencies leads to modeling obstructions as highly lossy or impenetrable, and adopting the assumption that reflecting surfaces or refracting regions are large compared to wavelength λ.

In the mid to lower HF, below the frequency range considered in this article, the very long range over the horizon propagation due to ionospheric interaction is unique. The troposphere and ionosphere reflectivity depend on relatively higher transmit power and antenna orientation. Here we focus on the upper HF and above, and consequently we ignore HF long range propagation while noting that under some conditions long range interference might be possible. Cognitive approaches can be employed to set up HF links and dynamically manage interference; e.g., see the extensive survey of spectrum inference and cognitive radio [49].

IV. LOW FREQUENCY PROPAGATION MODELING

Many of the benefits of using low frequency for autonomous systems come about by exploiting the propagation and penetration in complex environments. In this section we collect and review low-frequency propagation models and experiments. The propagation at long wavelengths has distinctive characteristics that differ from higher frequency, requiring different models than those widely employed in other bands. The low frequency propagation models support communications and networking, as well as other multi-robot processing.

Low frequency propagation modeling becomes nuanced, as the longer wavelengths enable penetration while at the same time less scattering occurs especially from smaller obstacles that are on the scale of the wavelength or less, and assumptions leading to ray tracing become inapplicable. The shift from multipath fading becomes more apparent as the wavelength becomes longer with decreasing frequency from UHF, to VHF, to the lower VHF and upper HF. In addition to the classical factors (e.g., transmit power, antenna height, range), low frequency propagation is also sensitive to the environmental complexity and material size and composition relative to the wavelength. Low frequency experiments and models describe sometimes very different cases and a variety of heuristic, statistical, and numerical models have been proposed. For practical reasons many older, traditional studies may pick a single frequency and define a model that is valid for that narrowband channel, but the model might not be accurate across a range of low frequencies.

Basic VHF propagation models often proceed by applying some form of regression to path loss measurements in various environments. These may span representative environment classes such as urban, open terrain, etc., and measurements are often taken outdoors only. The fitted regression model provides an average path loss versus range. The results are highly dependent on whether the antennas are elevated or ground level and the measurements are LOS versus NLOS. The most common low VHF studies are (i) motivated by broadcast from an elevated tower, with high power (W's to kW's) and long range (km's), or (ii) ground level, often referred to as mobile-to-mobile. A random component can be incorporated into path loss models, and statistical models have been developed for broadcast to predict coverage/outage.

More sophisticated VHF studies, as described below, go further and consider delay-spread, indoor and indoor-outdoor, building and structure penetration, ground wave, and low-power short-range. For very practical reasons, many propagation measurement campaigns can only sample a few frequencies, but this makes it difficult to discern the changes occurring when comparing, say, 40 and 100 MHz, where wavelength changes from 7.5 to 3 m and the environment may seem quite different in terms of scatterer size and spacing.[1]

Statistical models have also been developed in the lower VHF, building on the Rayleigh-Rician framework, and the parameters can be adapted as a function of frequency. Generally, penetration results in a LOS-like component, and low-VHF Rician models have been explored for some environments.

[1] We might compare with 1 and 2 GHz, where the wavelengths are 0.3 and 0.15 m, yet statistical propagation models are very similar.

A. VHF BROADCAST PROPAGATION MODELING

There are extensive historical studies of scattering, reflection, and ducting in VHF and UHF, for long range propagation modeling, especially beyond line-of-sight. As discussed in Section III, implementation of broadcast mobile radio resulted in many studies of elevated base station and near-earth mobile, with high transmit power and long range [47]. These were often motivated to predict coverage and blackout areas based on path loss. Broadcast television and radio have similarly motivated recent studies of path loss and coverage in urban areas, e.g., at 200 MHz [50]. A variety of empirical, heuristic, and geospatial path loss models have been proposed with transmit power in kW's and ranges of km's, e.g., urban TV broadcast at 89.3 and 103.5 MHz [51], while not necessarily including specific modeling of penetration into buildings. Similar studies have been carried out for HD radio in dense urban, e.g., path loss measurements at 103.3 and 95.7 MHz for high power and long range [52]. Due to the difficulty of finding heuristic models, neural networks have been considered in a variety of broadcast scenarios, especially for UHF, e.g., see the extensive survey in [53]. VHF path loss models for elevated towers to rooftops have been studied down to 30 MHz, based on modeling buildings as a series of dielectric screens [54].

B. MOBILE-TO-MOBILE PROPAGATION

A variety of ground based path loss models are available for HF, VHF, and UHF in various generic environment classes, typically for high power (W to kW) and longer range (km's), and these can be used to simulate coverage and outage, e.g., see [55]. UHF ground-based urban path loss modeling studies consider LOS and NLOS cases, e.g., using regression fitting; see [56] and references therein. Measurements in $30-88$ MHz have been used to modify path loss models with a random environmental factor to fit observed data [57]. A 2012 survey notes the lack of in-depth studies of ground-based urban path loss models in $30-88$ MHz [58].

The allocation and use of the lower VHF has been evolving, e.g., with the elimination of analog TV broadcast. VHF spectrum has become available in some countries for Internet of Things (IoT) and Machine to Machine (M2M) low bandwidth communications.[2] For example, in the UK spectrum within the $55-68$, $70.5-71.5$, and $80.0-81.5$ MHz bands can be used for Internet of Things (IoT) services and Machine-to-Machine (M2M) applications. Motivated by the newly available VHF spectrum, path-loss measurement studies have been conducted to compare VHF and UHF for IoT applications. Studies compare 70 with 869 MHz [59], and 37.8, 57.0 and 77.5 MHz from the VHF with 247.25, 312.0, and 370.0 MHz from the UHF [60]. In these studies log-distance plus shadowing path loss models have been fit to measurements in several environments, with varying antenna heights. This path-loss model is typically expressed as, e.g., see Sec. 1.3 in [59],

$$P_L = K + 10\gamma \log_{10}(d) + X_\sigma, \tag{1}$$

where K is a constant, γ is the path loss exponent, d is the distance, X_σ models shadowing as a log-normal random variable with standard deviation σ, and constants K and γ are typically estimated using linear regression. Model parameters vary with frequency and environment (and antenna height and other factors), and compared with UHF the lower VHF generally shows much less path loss, although VHF may have higher background noise that increases in urban environments.

1) DELAY SPREAD AND APPLICABILITY OF THE RICIAN MODEL

Some low earth propagation studies go beyond path loss. For example, a 2006 study at 37.8, 57.0, and 77.5 MHz was conducted in a semi-urban setting [61]. Not surprisingly, it was observed that delay spread increased with increasing frequency and with the presence of large metal-sided buildings in the test environment. The authors also noted that average delay spread nearly doubled for each fourfold increase in distance, with a wide range of delay spreads at ranges greater than 1 km. Lower VHF measured delay spreads are typically reported to range from 10's of nsec to 1 or 2 μsec. Increasing delay spread also was correlated with received power variation. Rician models were studied and the Rician K-factor was estimated. The Rician model was only rejected in favor of a Rayleigh model in roughly less than 12 % of the cases studied.

Another urban study measured power delay-spread at 37.8, 57.0, and 77.5 MHz, using a wideband waveform and regression [62]. Generally similar themes were reported: the delay spread is more concentrated towards the initial arrival, attenuation increases with more clutter, and delay spread increases as a function of range. Early arriving power measurements show more variation in a more complex environment. See also [63] for VHF and UHF mobile to mobile delay spread measurements in four different environments, and delay spread measurements and modeling in [60], with transmit power 34 to 40 dBm (2.5 to 10 Watts).

2) RICIAN TAPPED DELAY LINE VHF CHANNEL MODEL

A tapped delay-line model for low VHF mobile-to-mobile is developed by Vigneron and Pugh [64]. They measured mobile-to-mobile channel impulse response in four environments at 37.8, 57.0 and 77.5 MHz, using a 5 mega-chip per second (MCPS) channel sounding waveform. The authors note the change in wavelength effect on material interaction, and therefore consider each frequency separately. Spatial coherence is measured, showing high spatial correlation for 37.8 MHz over a third to a full wavelength, depending on the environment. In an urban environment, the received 37.8 MHz waveform is almost unchanged over 2 to 3 meters spacing, and this can be converted to a coherence time for a

[2]We do not consider low power inductive loop short range devices (SRDs).

given mobility rate. The authors develop a tapped delay line simulator model, where each tap has Rician parameters that are dependent on the time delay and the environment. Tables of estimated Rician K-factors are given for each case. The model is similar to classic wideband fading models such as Jakes, but now the taps are modeled as Rician. The authors hypothesize that at the lower VHF frequencies, the channel consists of relatively few paths due to the long wavelengths and resulting fewer interactions with scatterers, leading to the Rician behavior.

C. FULL WAVE NUMERICAL PROPAGATION MODELING

Full wave numerical modeling complements theoretical and statistical propagation modeling, and is especially useful at low frequency. Full wave modeling enables detailed study of penetration, diffraction, phase shift, spatial coherence, and other effects in complex scenes. While the basic physics are described by electromagnetic theory, closed form solutions for Maxwell's equations are generally not available in complex environments. Direct numerical evaluation of Maxwell's equations in rendered 3D scenes beyond a few wavelengths has been limited due to the computational complexity and need for high resolution 3D sampling. However, recent advances in computational electromagnetics in conjunction with high performance computer clusters have enabled large complex 3D scene evaluation, e.g., spanning 1000's of wavelengths using finite-difference time domain (FDTD) methods [65]. This approach includes electromagnetic material properties, insertion of antenna models, and provides channel amplitude and phase between any two points in the scene. Examples and applications of FDTD modeling are described in later sections.

D. GROUND WAVE PROPAGATION

Ground wave (sometimes referred to as surface wave) propagation has been classically characterized for frequencies below VHF, roughly 10 kHz to 30 MHz, e.g., a 2014 ITU technical report describes history and development of ground wave propagation models [66]. Vertically polarized ground waves prefer conductive surfaces such as seawater, and ground conductivity depends on soil type and moisture content. Studies of propagation over water show that water conductivity and ducting can provide long ranges even with relatively low power (Watts can yield 10's of miles under appropriate conditions); e.g., see [67] and [68]. Generally, ground loss decreases as the frequency is lowered. VHF ground waves are affected by undulating terrain but can travel significant distances.

Classical short range models with low antennas include LOS, ground bounce, and ground wave terms. However, when these conditions do not hold, e.g, with undulating surface or dense vegetation, then these models are insufficient. The effect of vegetation and snow can be accounted for and VHF propagation models with low-earth antennas have been developed that are asymptotically applicable with respect to range (roughly, 100's of meters or more) [69]. Several electrically small antennas for maximizing VHF ground wave propagation have been developed using a full-wave hybrid ground wave propagation model [70].

A semi-analytical propagation model has been developed for propagation through buildings, with near-earth antennas, that incorporates ground wave propagation effects [71]. This model has lower complexity compared with a more general purpose full-wave simulation, for a given building environment; see also [72] and [73].

E. LOW FREQUENCY PENETRATION INTO STRUCTURES

A distinct advantage of low frequency is penetration into structures, and classic studies in the upper VHF and UHF demonstrate that the penetration loss increases as the frequency increases, e.g., see Parsons [47, Chapt. 4]. Fundamentally, given a lossy dielectric slab (e.g., as a model for a wall), higher frequencies will experience more loss because the slab is thicker in terms of electrical size as the wavelength decreases. Also, the conductivity of dielectrics (such as concrete) generally increases as frequency increases, resulting in more electromagnetic energy dissipation.

A common classical urban path loss modeling approach assumes that loss is proportional to range d (say, d^4), with signal strength log-normally distributed, and may include a correction factor that depends on the environment, e.g., see Parsons [47, Chapt. 4.3], with a correction based on the extent of ''urban clutter''. While there are many comprehensive studies of microwave building penetration [74], there are fewer such low frequency studies.

Environments can be classified (e.g., dense urban, rural, etc.) and model parameters can be adapted to each case. Heuristic modifications may include urban characterizations such as building density, size, and material composition. These can be site specific, and models typically encounter the tradeoff between general application in a variety of environments versus more accuracy but with only site-specific applicability.

Motivated by emergency response scenarios, signal strength measurements into large buildings taken over a variety of structure types across frequencies from 49 MHz to 4.9 GHz show a large variation and do not readily match a particular statistical model; see [75] and references therein. A unique companion study measured signal strength into buildings before and after collapse, and the results show a generally increasing attenuation and high variability after collapse, although enhancement of propagation is possible in some cases [76]. Other penetration studies include upper VHF and UHF building penetration for short range emergency response [77], [78], and LEOS penetration at 137 MHz [79].

Full wave simulations (Section IV-C), enable studies of penetration that incorporate specific building layouts and materials. Simulations of modern glass and metal high rise buildings show how periodic metal rebar in reinforced

concrete can act as a high pass filter and suppress low frequency propagation [80], while between floors may act as a waveguide as if the building is relatively transparent; see [81] with VHF-UHF simulations. A related study considers rebar blocking and building materials [82].

F. APPLYING LOW FREQUENCY PROPAGATION MODELS

Depending on the application and desired fidelity low frequency propagation modeling and prediction may require careful consideration of the environment including the effects of penetration, diffraction, reflection, waveguide type behavior through some metallic structures, ground bounce when elevated, ground wave, and the potential for electromagnetic coupling between the antenna and the environment or platform.

Simple ray trace methods are inapplicable, so numerical methods rely on direct calculation of fields using Maxwell's equations. Numerical modeling in complex scenes, especially using recent advances in FDTD, is important for understanding penetration and phase alteration. Large scale 3D scenes can be complex to numerically evaluate, although it can be expected that advances in computing will continue to enable larger and more complex modelng to be explored. Generally, the computational complexity scales with the geometry in terms of the number of wavelengths covered.

A variety of studies have confirmed the remarkable penetration achieved with low frequencies in urban scenarios as the wavelength extends to meters. Direct comparisons with microwave and low VHF highlight this difference. The Rician statistical channel model appears to be reasonable for many scenarios and NLOS channels can have a relatively strong K factor based on penetration, whereas at higher frequencies this tends to occur only in LOS channels. Near earth wideband studies show reasonable fit to the Rician model with relatively sparse time delayed terms. The low frequency channel delay spread can be quite small for short range narrowband channels, and numerical studies of dense urban channels support this conclusion. At long wavelengths the lack of sufficiently large reflectors, and a relatively small fractional bandwidth, yield a short range channel that has little frequency selectivity. The resulting small channel phase variation across frequency can be exploited in code design for low frequency CDMA (see Section X).

Low frequency propagation tends to have a relatively smooth spatial power decay. This is much different than higher frequencies that are dominated by multipath and, hence, the received signal strength (RSS) has much higher spatial variation. Consequently, low frequency spatially separated RSS measurements can be used to infer geometry and direction (see Section VII).

There are relatively few studies that consider spatial statistics in complex scenes. Numerical studies and experiments indicate that narrowband array processing and beamforming techniques can be adopted, although good models for spatial phase correlation are not available. Studies of phase front expansion in urban scenes indicate that small scattering effects may cause local phase change that is relatively smooth, at least for relatively short range propagation. Consequently, classic narrowband beamformers can be applicable although the phase relationship measured across an array will not necessarily correspond to that expected in free space for the same geometry (see section VIII and references therein).

Low frequency propagation modeling is further affected by the specific wavelength. Progressing through the VHF band from 30 to 300 MHz, the wavelength shrinks from 10 to 1 meter, and consequently the interaction with objects and materials can be quite different. Numerical indoor/outdoor studies show considerably more short range phase alteration at 100 MHz ($\lambda = 3$ m) versus 30 MHz ($\lambda = 10$ m). These effects are relative to the environmental makeup such as wall spacings and presence of metal beams and metallic frames, aperture sizes relative to the wavelength (e.g., windows, large entryways), elevation and ground bounce, as well as ground wave for near-ground antennas.

The propagation is also complicated by metallic objects near the antennas, including the platform an antenna may be mounted on, due to electromagnetic coupling. The coupling becomes significant when objects are within a distance that is a relatively small fraction of the wavelength, but with meters-long wavelengths it becomes much more likely that metallic objects will be close enough; see also Sections VI and VIII.

V. SHORT-RANGE COMMUNICATIONS

In this section we focus on the short range case in densely cluttered environments. Section V-A reviews short range propagation studies, and section V-B describes low power short range communications experiments.

A. SHORT RANGE PROPAGATION

Several studies have considered low-frequency short-range propagation in cluttered indoor/outdoor environments with an eye towards autonomous systems [83], [84], [85].

A study of the viability of low-power short-range low VHF communications was carried out through measurements and analysis in indoor/outdoor cluttered environments [83]. Measurements and full wave simulation studies were conducted for indoor and indoor/outdoor cases, with a maximum transmit power of 32 mW. In order to make the channel measurements more efficient and enable collection of large datasets, a short dipole antenna ($\lambda/6$) and software defined radio receiver were mounted on a small unmanned ground vehicle (UGV) that was tele-operated over extended indoor/outdoor environments. This included indoor collection up to 40 m range in LOS and NLOS conditions, and outdoor testing with buildings and metallic structures up to 200 m range. Channel sounding with tone and pulse-based waveforms was conducted. Propagation analysis included channel transfer function estimation, measuring phase distortion compared with a wired reference signal, and hypothesis testing for the presence and level of multipath

based on phase and amplitude statistics. In the cases studied, the channel phase distortion and multipath were minimal and typically statistically insignificant, and the narrowband channel could be reasonably modeled as a simple delay with scalar attenuation and additve white Gaussian noise (AWGN).

A related study of low-power short-range propagation compared 40 MHz and 2.4 GHz propagation [84]. Measurements for indoor-to-indoor, outdoor-to-indoor, and non-line-of-sight outdoor scenarios were used to quantify and compare 40 MHz and 2.4 GHz channels. For each measurement scenario considered, path loss and small-scale fading were characterized after carefully calibrating the differences in the systems used for measurements at different frequencies, including variations in antenna performance (because electrically small antennas were used at the lower frequency while half-wave dipoles were employed for the higher frequency measurements). For all the scenarios tested, it was shown that the path loss at 40 MHz was on average 40 dB less than that of the 2.4 GHz case. Ranges varied across the scenarios, up to a maximum range of 76 m, corresponding to about 10 wavelengths at 40 MHz. The measurements showed that even in highly cluttered environments (in the presence of dielectric and metallic obstacles), the propagation mechanisms at 40 MHz and 2.4 GHz are very different. Low frequency penetration through many building walls is possible because of the relatively small electrical size of typical scatterers compared to the meters long wavelength. In contrast microwave propagation was dominated by multipath with much less penetration.

B. SHORT-RANGE COMMUNICATIONS EXPERIMENTS

The propagation studies described above showed the viability of low-power low frequency using sub-wavelength antennas in cluttered environments, and indicated that the short-range narrowband propagation channels may be very benign [83], [84]. Next we consider short range communications in these environments.

Short range low power ($\approx$ 5 mW) communications experiments were carried out using a full-duplex frequency conversion circuit to mix a low cost commercial ZigBee radio down to 40 MHz for transmission, and mixing back to the 2.4 GHz ZigBee device passband at the receiver [86]. Experiments were carried out in complex non-line-of-sight indoor and urban-type indoor/outdoor scenarios. For comparison, a similar commercial radio at 2.4 GHz was used in the same scenarios. Example results are displayed in Fig. 1, showing received signal strength (RSSI) and packet error rates (PER) versus range, where the measurements were taken along a path that begins indoors and extends outdoors. The penetration is evident in RSSI and PER for the low frequency link. The predicted free space loss is also shown, and the low frequency measurements indicate a very similar trend despite the penetration. The results demonstrate that compact, low-power, low-frequency radios can provide more reliable and persistent communications compared to 2.4 GHz,

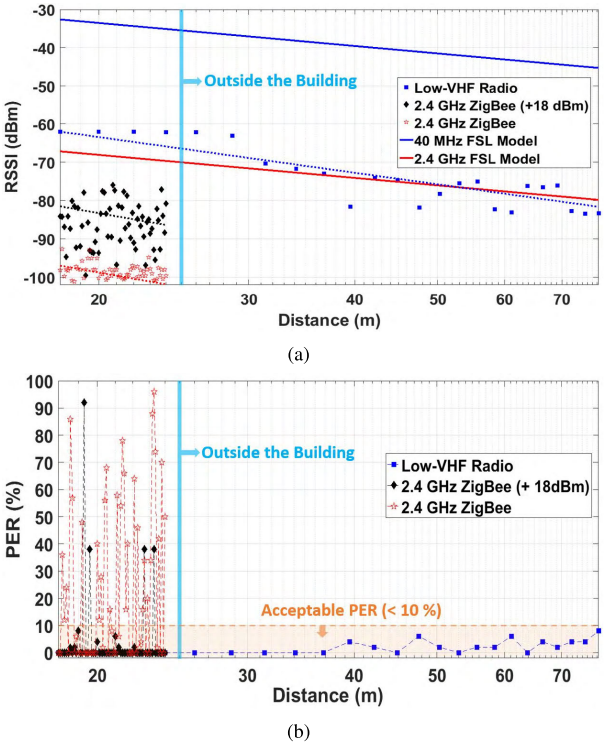

FIGURE 1. Results from an indoor/outdoor communications experiment from [86], contrasting low frequency (40 MHz) and 2.4 GHz. The transmitter was located indoors, and measurements at different ranges are shown with (a) average RSSI, and (b) packet error rate (PER). The measurements progress from indoors to outdoors at a range of 25 meters. Predicted free space loss (FSL) trends are also shown, and the 40 MHz RSSI follows the predicted free space trend despite the penetration through the building. A 2.4 GHz ZigBee radio with higher transmit power (+18 dBm) is also shown, with highly fluctuating PER indoors due to multipath fading, and very low RSSI outdoors due to poor penetration through the building walls.

with much longer range and penetration at the same transmit power.

Short range video webcam streaming experiments were conducted at 40 MHz using software defined radios, with the transmitter mounted on a small UGV navigating inside a building and communicating to an outdoor receiver [87]. Transmit power was limited to $<$ 20 dBm. Video frame compression/decompression and digital modulation/demodulation were carried out in software, and video quality and bit error rate were evaluated in a variety of geometries. Compression was needed to reduce the data rate, but signal processing was kept to a minimum in order to study the channel effects. Typically applied communications processing techniques were omitted, such as channel equalization, dynamic control, forward error correction, and coarse frequency offset compensation. The results demonstrated that the channel was sufficiently benign in a majority of geometries to enable video transmission with very simple receiver processing.

VI. ANTENNAS

Small antennas are a key enabling technology for mobile autonomous vehicles. For the low frequencies considered here with corresponding meters-long wavelengths, a small

antenna aperture is sub-wavelength in extent, and this leads to design tradeoffs. We refer the reader to a recent comprehensive survey of small low-frequency antennas, highlighting recent progress and applications to robotics and autonomous systems [88], and limit our discussion here to basic issues and ideas.

Passive linearly polarized electrically small antennas (ESAs) are subject to an upper bound on the product of the fractional-bandwidth and radiation-efficiency, referred to as the Chu-Wheeler limit. An example is shown in Figure 2. The limit is expressed as a function of the product of (i) the smallest possible sphere of radius a that can fully enclose the antenna, and (ii) the free space wavenumber $k = 2\pi/\lambda$. As $a \ll \lambda$, i.e., the antenna becomes very small, then maximum efficiency suffers as shown in Figure 2. Note that the bound is a product of bandwidth and efficiency, so that small antennas with high efficiency tend to become more narrowband. Many design variations have been studied, including designs that fill a 3D volume (such as rectangular shaped), and retunability to achieve near optimal efficiency at different center frequencies [88].

The meters long wavelengths can also result in electromagnetic coupling between the antenna and metallic objects in the environment. In many scenarios nearby objects can easily be close enough to induce coupling. The coupling can be exploited in platform integrated antenna designs, resulting in a larger effective aperture; several such designs are described in [88]. Low-earth small antennas can also be designed to provide an enhanced ground wave through coupling, e.g., for sensor networking applications [70]. Coupling can also be exploited in compact low frequency antenna arrays, as discussed in Section IX. On the other hand, coupling with nearby objects in the environment can change the antenna response in an uncontrolled way.

The Chu-Wheeler limit holds for passive antennas, but it is possible to enhance the antenna performance (especially the bandwidth) without changing the form factor by using active matching circuits. The matching circuit requires a power source and so the antenna is no longer referred to as passive. Passive designs often utilize LC circuits for matching, while active non-Foster circuits enable bandwidth-enhanced operation at the expense of power consumption. It has been demonstrated that for small aperture size a, it is possible to enhance the bandwidth beyond that achieved by a similarly sized passive low frequency antenna [88], [89].

VII. GEOLOCATION

This section describes recent progress on geolocation methods that exploit low frequency propagation in cluttered environments. Section VII-A sets the context with a high level review of multi-robot localization, mapping, and geolocation. Multi-robot teams rely on these techniques that underpin the ability to collaborate in complex scenes, and the use of low frequency can enhance network connectivity, enable collaborative geolocation, and provide spatial information such as bearing angle to a source. Similar to the communications

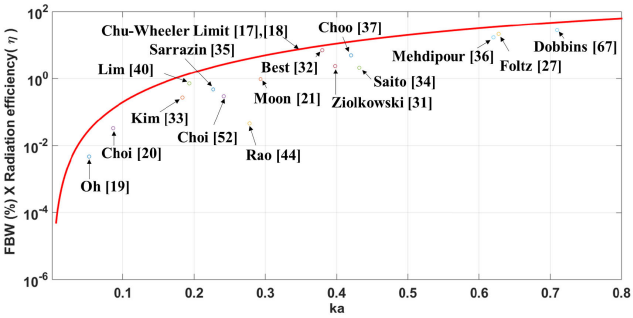

FIGURE 2. The Chu-Wheeler bound on passive antennas expresses an upper limit on the attainable fractional-bandwidth radiation-efficiency product as a function of the product of the aperture a and the wavenumber $k = 2\pi/\lambda$. As the physical size a becomes much less than the wavelength, the achievable bandwidth-efficiency product is reduced. The figure and design citations are from [88]. ©2022 IEEE.

scenarios explored in other sections of this article, the penetration and propagation of low frequency signals can be exploited in challenging environments. Geolocation is a foundational tool for autonomous systems that can be used to aid navigation, sensing, and communications, and the techniques described below can readily combine with agent mobility and multi-agent collaboration.

Classic narrowband plane-wave free-space angle of arrival estimation between two or more antennas is based on measuring the time delay or carrier phase difference between the antennas. This can be accomplished in some complex environments at low frequency, as described in sections VII-B and VII-C. The received signal strength (RSS) can also be exploited to infer source direction from spatially separated samples. This is described in section VII-E.

A. MULTI-ROBOT SLAM AND GEOLOCATION

Simultaneous localization and mapping (SLAM) relies on autonomous exploration and robot perception to create a map and self-localize in the map. Multi-robot systems use networking for collaborative SLAM, and coordination strategies can be employed for efficient exploration and mapping [90]. Advances in visual perception based on neural networks have led to SLAM methods that rely on vision [91], whereas many traditional methods rely on range estimation, e.g., using LIDAR. Various active and passive sensor modalities can be used to enhance overall performance, and these can be combined with semantic information in a variety of ways [92]. Active SLAM couples perception and navigation to intelligently navigate and gather information during the exploration and mapping. A recent survey describes classic and emerging methods for active SLAM [93]. Overall, the use of low frequency for multi-robot SLAM is motivated by the need for network connectivity to enable collaboration.

There are many geolocation methods for locating, ranging, and tracking a low frequency source, and this may be cooperative between agents or for the purpose of geolocating a low frequency source in the environment. Thus, low frequency geolocation methods can be used for robot collaboration,

as well as to localize a source of interest. Cooperative localization methods have been extensively studied for sensor networks [94], and these can be adopted for multi-robot systems.

Ultra-wideband (UWB) has been explored for collaborative multi-robot localization [95], [96], especially for indoor short-range scenarios using two-way time-of-flight estimation [97]. Indoor multipath propagation induces pulse spreading that complicates the receiver processing and reduces the potential ranging accuracy that could be achieved with an undistorted pulse, and protocols may use multiple two-way transmissions to reduce ranging errors. While UWB can be effective in short range scenarios, it is limited by low power transmission and the resulting delay spread in the wireless channel that may severely distort the received pulse shape. UWB receivers are also susceptible to co-channel interference from other emitters in the same spectrum band because they have such a large receiver bandwidth.

Two-way time of flight ranging is more effective for line of sight channels where the propagation is more favorable. For example, two-way time of flight ranging for UAVs can provide localization and synchronization to support autonomy and networking [98], [99].

B. PHASE DISTORTION IN COMPLEX ENVIRONMENTS

Phase-based angle of arrival estimation typically assumes that the propagation environment is homogeneous, so that the narrowband signal phase simultaneously measured at different spatial locations can be used to infer wavefront propagation direction. As described in section IV-E, low frequency signals are able to penetrate structures and obstacles. In general, when compared to the free-space case, propagation in a non-homogeneous environment will result in phase variation and distortion as a function of propagation angle and this spatial phase variation violoates the free-space model. However, in some cases, depending on the frequency, environment, and propagation range, the phase distortion may be small enough such that phase-based angle of arrival estimation can be effective based on a free-space model. Array processing in the non-homogeneous propagation case is considered in Section VIII.

Full-wave EM simulations have been used to study how building penetration leads to phase variation that differs from propagation in free-space [65]. To illustrate the effects of penetration on signal phase, we present a full wave EM simulation in the environment shown in Figure 3, with 7 buildings of varying sizes. Each building consists of 4 walls and a ceiling, and four solid towers are also included. The walls, ceilings, and solid towers are modeled as homogeneous dialectric slabs made of concrete. A near-ground transmitter is positioned at the center of the scene and transmits a tone at the center frequency of interest. The complex signal is densely sampled on a plane parallel to the ground at the same height as the transmitter using the full wave FDTD solver [65]. The simulation was repeated at 12 distinct

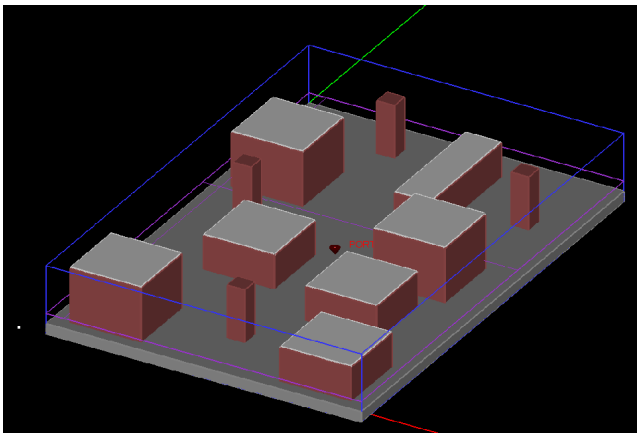

FIGURE 3. Multi-building 3D model for the low frequency propagation simulation described in Section VII-B, for studying the effect of penetration on low frequency signal phase. Building walls and ceilings are modeled as homogeneous slabs of concrete. An outdoor transmit antenna is pictured in the center of the scene. Low frequency propagation results are shown in Figure 4.

frequencies ranging from 10 to 200 MHz. As a baseline for comparision the simulations were repeated with only the ground (without the buildings).

Two-dimensional propagation phase plots at 40 MHz are shown in Figure 4, where the transmit antenna is located at the origin. Only the phase is plotted, without accounting for amplitude reduction. In free space (top of Figure 4) the expected circular expansion is evident. With the ground only (middle of Figure 4), the phase front is visually very similar to the free space case. When the buildings are introduced (bottom of Figure 4) some phase aberration becomes apparent, and this is especially pronounced at the tower locations.

To investigate the amplitude and phase distortion in the buliding environment, samples were collected around circles of fixed range from the transmit antenna. For a given range, phase and amplitude distortion around the sampled circle were measured by the standard deviation of phase (in degrees) and amplitude (in dB), respectively. In free space there should be no variation in phase or amplitude around a constant range for any propagation angle. The results are plotted in Figure 5, with amplitude distortion vs range in the left side column, and phase distortion vs range in the right side column. Range was sampled from 15 to 40 meters, and the results are parameterized by frequency.

This example shows that the phase and amplitude distortion increase as a function of range and frequency. The amplitude distortion shows a generally linear trend with range, and is relatively small in the 10 to 40 MHz cases (upper left panel in Figure 5). The phase distortion reveals that at some specific ranges the variation becomes pronounced, observed as outliers in the plots, and the occurence of outliers increases with frequency. In the 10 to 40 MHz cases (upper right panel), the 10 MHz case has no outliers, and the other cases show increasing outlier occurence.

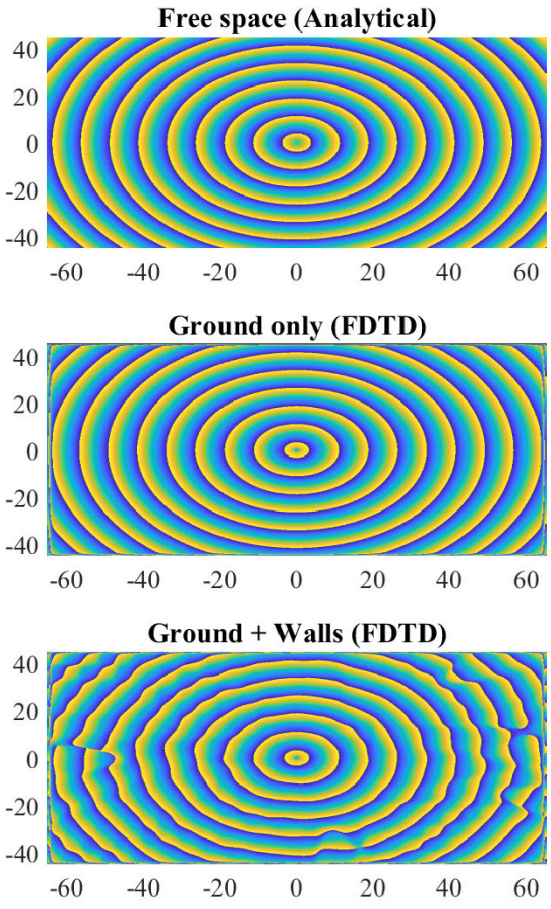

FIGURE 4. Low frequency propagation example in the environment shown in Figure 3, described in Section VII-B. The plots show the signal phase for a simulated transmitted single frequency signal, with the antenna located at the origin. From top to bottom, the phase front for the free space case (analytical), ground only (simulated), and with buildings (simulated) are shown. The phase abberation due to the buildings is evident.

At higher frequencies the overall phase variation increases dramatically, even for the lowest range.

C. ANGLE OF ARRIVAL ESTIMATION

Phase-based angle of arrival estimation in highly cluttered environments was studied in [100], including full-wave propagation modeling from 5 to 100 MHz, and experiments at 20 and 40 MHz. This study focused on measuring the phase-offset between two antennas for short range through-building estimation of angle of arrival of a narrow-band source. Highly miniaturized omni-directional vertically polarized antennas were used to demonstrate angle estimation through buildings.

The frequency choice for accurate angle estimation depends on the environment and the desired range of operation. Full wave 3D modeling was used to determine the highest frequency at which the error was within a desired tolerance, and the simulation environment was altered by adding walls and ceilings [100]. The results generally favored meters long wavelengths with frequency around 20 to 40 MHz, similar to those in the simulation described in section VII-B. At 100 MHz the signal components scattered by the building walls, ground and ceiling become comparable to the direct field component causing significant fading and uneven field distribution, such that phase-based angle estimation assuming a free-space model will be ineffective.

D. TIME OF ARRIVAL BASED GEOLOCATION

The potential for utilizing low frequency time-of-arrival based ranging for geolocation of a mobile node has also been investigated [101]. Full wave simulations were carried out for a cluttered indoor environment, incorporating polarization diversity and multiple anchor receivers to jointly geolocate a mobile emitter at 20 and 40 MHz. An empirically derived effective dielectric constant was used for penetration delay compensation, resulting in predicted sub-meter geolocation accuracy.

Although outside the scope of this article, ground penetrating radar for subsurface imaging is an important application. Penetration is improved at longer wavelengths, although this generally leads to a loss of imaging resolution so there is a tradeoff with using lower frequencies. However, wideband VHF waveforms can be used for imaging, using measurements from multiple locations [102], [103], [104], [105].

E. RSS-BASED PROCESSING

Received signal strength (RSS) is easily measured and can be exploited to provide relative spatial information between the source and the receiver. At low frequency the RSS has a relatively smooth spatial decay as the range from the source increases. This is in contrast to higher frequencies that are subject to multipath fading in cluttered environments, resulting in high spatial RSS variance with small spatial separation between measurements. The low frequency RSS decay with increasing range enables RSS-based geolocation and source tracking in complex environments. Spatially separated RSS measurements can be used to estimate the RSS spatial gradient and then infer source direction in two or three dimensions. This has unique advantages including (i) not requiring knowledge of the source power because only a relative spatial RSS change is measured, (ii) ability of a single agent to move and collect RSS samples and thereby infer angle of arrival, and (iii) the method does not require a highly calibrated RSS sensor.

Note that, although geolocation can be inferred from multiple separated RSS-based range estimates, direct estimation of range from RSS measurements is challenging and requires both a highly accurate path loss model and power calibration between the source and the detector. Small inaccuracies in either the propagation prediction or the transmit power can result in large range uncertainty.

Next we describe two approaches to estimating and exploiting the RSS spatial gradient that have been developed

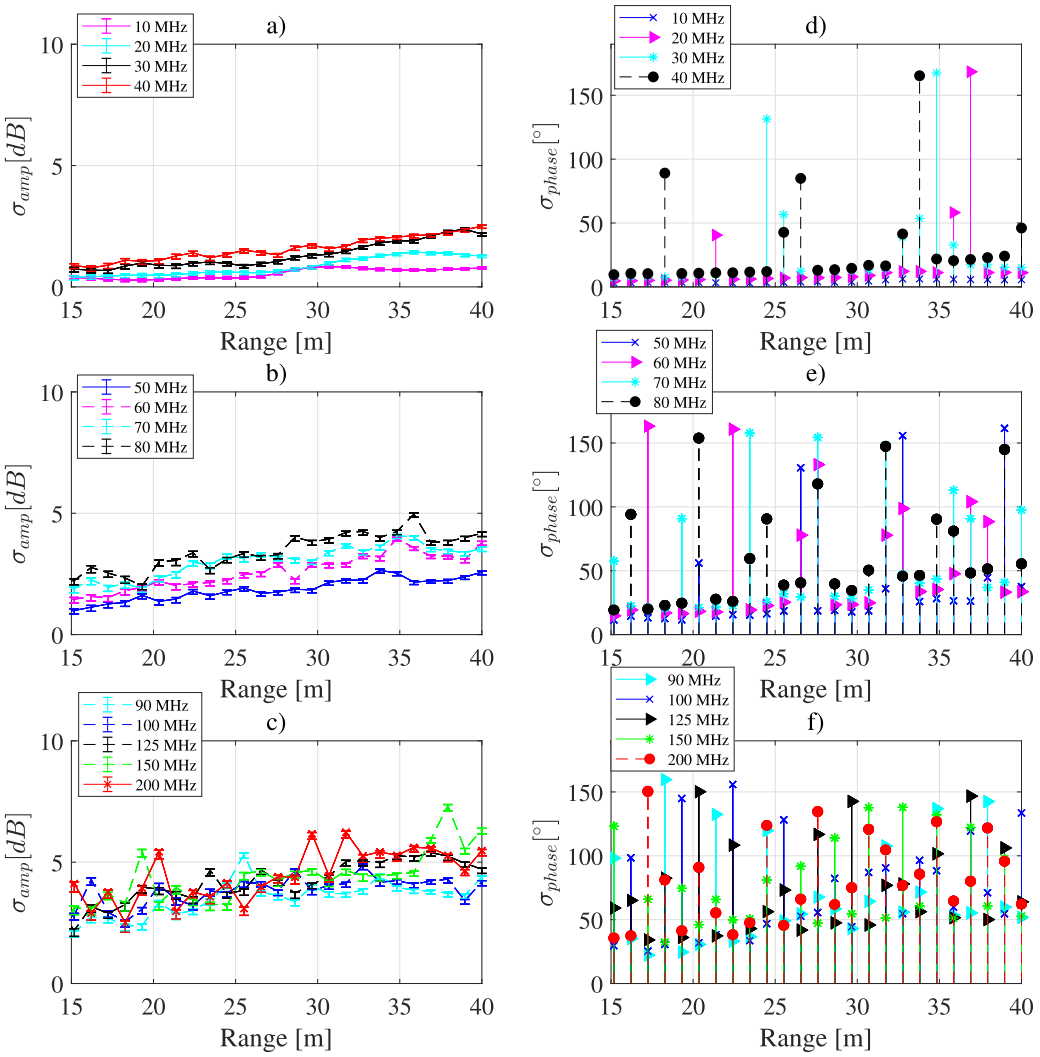

FIGURE 5. Simulated propagation results from the non-homogeneous environment shown in Figure 3, and described in Section VII-B. The amplitude and phase distortion are measured using the standard deviations of the amplitude (in dB) and phase (in degrees) for a fixed range around the transmitter. In homogeneous free space there is ideally no variation in amplitude or phase at constant range.

recently. First, collecting RSS samples in a spatial region and estimating the 2D (or 3D) spatial gradient, and second, we describe a more sophisticated Bayesian approach. These can be coupled with mobility for adaptive spatial RSS sampling, source geolocation, and source tracking. Both of these approaches can be used at higher frequencies in fading environments, e.g., microwave frequencies, although this generally requires more spatial samples and smoothing to overcome small scale fading.

1) RSS AND MOBILE SAMPLING

Several studies have explored the collection of RSS samples on autonomous air and ground vehicles, and using these RSS samples to estimate the RSS spatial gradient. The spatial gradient is then exploited in autonomous control for various purposes. These studies typically consider microwave (2.4 GHz is common), and it is reasonably expected that they can be applied using low frequency and benefit from the penetration and lower levels of multipath-induced RSS variation.

Estimating the RSS spatial gradient requires sufficient local sampling to smooth over local variations, especially small scale fading that may produce large RSS fluctuation. This question is studied in detail in [26] and [106]. Given RSS samples, plane fitting can be adopted to estimate the 2D gradient and infer source direction. In [106] this approach is coupled with robot exploration of a previously unknown environment and simultaneously moving toward a radio source. In [26] the spatial gradient is used to autonomously find the connectivity region of a base station, where connectivity is defined as the region where the received RSS is above a threshold. The control algorithm efficiently discovers the threshold region using the RSS spatial gradient by criss-crossing the boundary around the RSS threshold.

Additional studies consider using RSS for an autonomous unmanned air vehicle (UAV) to move towards a source [107], and tracking the RSS gradient among mobile agents to detect relative motion towards or away from each other and using this to move and preserve connectivity [22].

2) BAYESIAN RSS GRADIENT PROCESSING

The plane-fitting approach based on RSS samples described above can be effective, but has two drawbacks. The RSS gradient measurements can be noisy due to statistical variation and tend to be less accurate with small local spacing, and they may be spatially correlated due to variations in the propagation environment. To deal with these challenges in a principled way a Bayesian approach to RSS-based angle of arrival estimation was developed that produces an informative uncertainty estimate factoring in the sampling geometry as well as noise in the model fit [108], [109]. This builds on the success of the plane-fitting ideas discussed in the previous subsection with improved accuracy and robustness. The Bayesian approach is appealing for this problem because it incorporates uncertainty quantification that can be used to inform a mobile agent.

The RSS measurements are assumed to follow a log-distance path loss, a commonly used RSS model as a function of distance over a large range of frequencies, including both shadowing and small scale fading terms. RSS measurements are then modeled as locally linear [108],

$$\mathbf{y} = \mathbf{X}\beta + \epsilon \tag{2}$$

where $\mathbf{X}$ contains the 2D RSS sample point positions, β is the RSS gradient vector, and the entries of the vector ϵ are zero-mean Gaussian with variance σ^2. While the 2D RSS surface is generally not linear, the surface becomes increasingly planar locally as the distance d from the source increases. It is shown that the second derivative terms are of order $1/d^2$, and so they decay rapidly [108]. The gradient magnitude has an inverse relationship with distance to the source, and so it becomes smaller and therefore more difficult to accurately estimate as d becomes large. The Gaussian assumption on ϵ follows because the (log) noise arising from both shadowing and Rayleigh/Rician fading is well approximated by a normal random variable.

Using (2) a Bayesian linear regression algorithm is set up for estimating β and σ^2. A prior on the noise variance σ^2 can be selected based on measurement campaigns that have been conducted measuring RSS at various frequencies and environments. Under the above assumptions the marginal posterior on β is a Student-t distribution that is well approximated by a multivariate Gaussian for large enough sample size. The posterior on σ^2 indicates how much fading and shadowing are affecting a set of RSS measurements. If this value is large then the angle estimation will be poor, and remediation steps can be implemented, such as collecting more samples. The mean and covariance of the posterior on β provide statistics of the spatial gradient estimate that also illuminate the angle estimation accuracy.

The Bayesian inference algorithm in [108] is preceded by locally adaptive data clustering/aggregation to remove spatial autocorrelation and improve the statistical fit of the subsequent Bayesian plane fitting procedure, and also includes an outlier detection and removal step. These are shown to significantly enhance the overall performance.

The method was tested with various datasets at microwave and low VHF frequencies, with generally very good results. As expected, the angle of arrival estimates at large distances d from the source had smaller error (and smaller uncertainty) at lower VHF relative to microwave. Figure 6 illustrates the key ideas using RSS samples of an office building environment at 40 MHz from an FDTD simulation. Figure 6(a) shows an estimated angle vector (blue arrow), associated uncertainty (dashed blue ellipse), and true direction (black arrow). The RSS was sampled uniformly within the red region, and the median of the sampling region is shown as a green dot. The x and y axes denote the distance in meters from the source as measured along each axis. Note how the angle uncertainty estimate fails to cover the true angle, because the result in (a) has not included the clustering and outlier removal steps. Panel (b) shows a heatmap of the residuals of a planar RSS fit, revealing strong spatial auto-correlation. The algorithm progressively clusters and averages data locally until the residuals fail to show a statistically significant level of dependence, and the results are shown in panel (d) with residual magnitudes reduced. The resulting estimate is shown in panel (c); the algorithm provides an uncertainty estimate that includes the true angle.

VIII. MULTI-AGENT DISTRIBUTED ARRAY PROCESSING

In this section we consider low frequency distributed array processing where the antenna elements are physically separated without wired connection. Distributed array processing can take advantage of the penetration through dense environments such as buildings (Section IV-E), and miniature antennas (Section VI), and is appealing for multiple robots to collaborate and form an array.

A. MULTI-AGENT DISTRIBUTED BEAMFORMING

Distributed beamforming consists of separated antennas that collaboratively form a beam for transmitting or receiving radio communications [110]. This can be implemented among a multi-agent collaborative group, each with it's own antenna and transmitter, enabling high power directional communications. Key challenges for coherent distributed beamforming include timing and carrier synchronization [111], where increasingly accurate synchronization is required as the frequency increases. Residual phase errors arise with imperfect synchronization and noisy channel state information (CSI) [112]. Operating at low frequency significantly relaxes these synchronization requirements.

Low frequency distributed beamforming is especially appealing with multiple autonomous ground or air vehi-

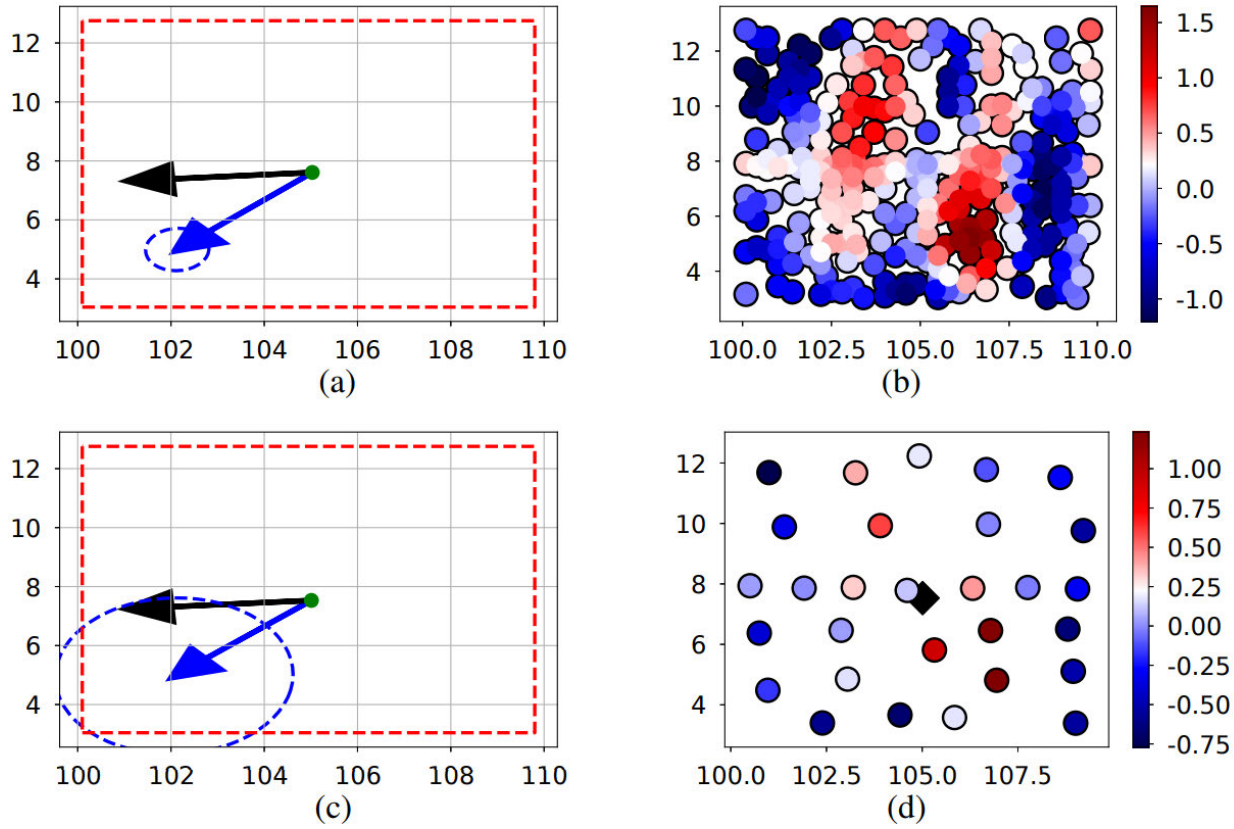

FIGURE 6. Bayesian angle of arrival estimation using the received signal strength (RSS) spatial gradient (Figure 13 from [108]). Panels (a) and (c) show the true angle to the source (black vector), and the estimated angle to the source (blue vector). The Bayesian estimator also provides an uncertainty ellipse for the estimated angle, shown as blue circles. The mobile agent can reduce the uncertainty by collecting more RSS samples at different locations, and the algorithm also removes outliers. Panels (b) and (d) show spatial sampling and illustrate outlier removal. See section VII-E2 for more details.

cles (UGVs and UAVs). These can carry miniaturized sub-wavelength antennas (see section VI and review article [88]), operate in complex indoor-outdoor environments, and form ad hoc arrays.

Distributed beamforming solutions can be achieved with open or closed loop approaches, i.e., with or without feedback from the receiver. When the array is fully characterized geometrically, then a beamforming solution can be obtained directly in a one-shot solution. Alternatively, when a sufficiently accurate one-shot beamforming solution is not available then an iterative closed-loop approach can be used to refine the beamformer solution and achieve a target SNR at the receiver.

Classically the precise locations of all antenna elements would be known relative to each other and within a global frame of reference. Autonomous agents can self-localize, e.g., UGVs using collaborative simultaneous localization and mapping (SLAM) to orient themselves. However, in general there will be some residual localization error after executing a SLAM algorithm so that an open loop beamforming solution that assumes perfect location information will have some error.

The impact of localization error on one-shot (non-iterative, open loop) distributed beamforming is analyzed in [113] and [114]. The agents self-localize and form an array to transmit a common message to a far-field receiver. A risk-sensitive discrete optimization problem is set up to choose an agent subset for distributed transmission so that the desired signal-to-interference-plus-noise ratio (SINR) at the receiver is attained with minimum variance. Under the assumption that the agents have Gaussian localization errors, three one-shot algorithms were developed: Greedy, Double-Loop-Greedy (DLG), and Difference-of-Submodular (DoS), each of which chooses a subset of agents to optimize the quality-of-service without requiring feedback from the intended receiver [113].

When the localization errors for all agents are below a certain error variance threshold, the Greedy algorithm globally minimizes the variance of the SINR received by the base station while guaranteeing that the expected SINR is above a desired threshold. The DLG algorithm improves the empirical performance over the Greedy algorithm. The DoS algorithm enables the agents to locally optimize the reliability of the communication link even when the localization errors are large.

It is shown that when the agent localization errors have relatively small variances, characterized in terms of the carrier frequency, then the Greedy algorithm that chooses the agents with the lowest localization error variances will globally minimize the variance of the received SINR. The tolerable localization error variance is relative to the wavelength, and low frequency operation relaxes the localization error requirements, e.g., an error within one m^2 is considered relatively small at 40 MHz ($\lambda = 7.5$ m). This localization error is well within robotic SLAM algorithm capability in practice.

B. DISTRIBUTED BEAMFORMING WITH FEEDBACK

As discussed above, if localization information is available then an open-loop one-shot beamforming solution may be viable if the error is sufficiently small, as characterized in [113]. An alternative is an iterative approach that incorporates broadcast feedback from the receiver in order to adaptively improve the beamforming solution [115]. In general the solutions do not assume prior localization, and are gradient free. They can be performed in a fully distributed fashion, i.e., each agent identifies its beamformer phase without having knowledge of the other agents locations and phase components. They iteratively explore random solutions and retain the best one based on the client feedback.

Distributed array calibration can also be achieved by using an auxiliary node that is nearby and collaborates. A practical calibration procedure for coherent open-loop beamforming is developed in [116]. Each node communicates with the auxiliary node to synchronize and resolve uncertainty in the desired beam. Simulations and experiments demonstrate the pacticality of the method.

A simultaneous distributed beamforming and nullforming scheme is developed in [117]. A group of agents collaborate to send a message to a client using feedback-based beamforming, while simultaneously transmitting artificial noise with null-steering to the client. With the artificial noise, the SINR at the client is given by

$$\gamma = \frac{|\sum_{i=1}^{N} \sqrt{P_{B,i}} h_i e^{j(\theta_i + \phi_{B,i})}|^2}{|\sum_{i=1}^{N} \sqrt{P_{N,i}} h_i e^{j(\theta_i + \phi_{N,i})}|^2 + \sigma^2}, \tag{3}$$

where N is the number of agents. Here, $P_{B,i}$ and $P_{N,i}$ represent the transmit powers for beamforming and nullforming, and $\phi_{B,i}$ and $\phi_{N,i}$ are the phase components at agent i for beamforming and nullforming, respectively. The channel gain and phase between agent i and the client are h_i and θ_i, and σ^2 denotes additive white Gaussian noise (AWGN) power. The beamformer and the null-steering phases ($\phi_{B,i}$ and $\phi_{N,i}$) and powers ($P_{B,i}$ and $P_{N,i}$) are simultaneously adapted, so that the client will not be affected by the artificial noise whereas an eavesdropper may have degraded SINR. To test the distributed beamforming low-VHF channels were simulated in an urban scene with numerical full-wave propagation modeling [117].

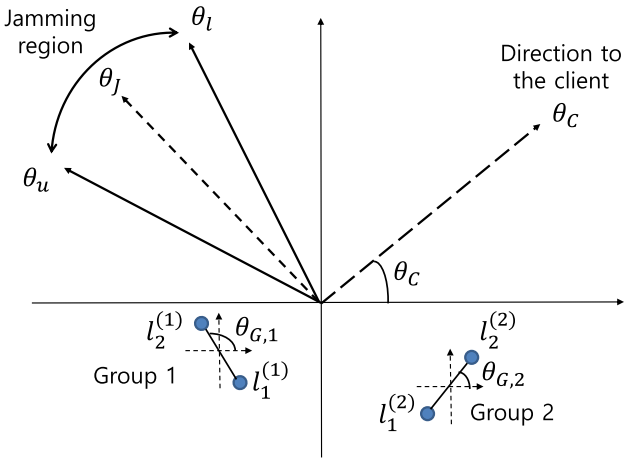

FIGURE 7. Multi-group distributed beamforming example, from [119]. Each group optimizes it's rotation angle θ_G to transmit artificial noise over a jamming sector $[\theta_l, \theta_u]$ with null-steering to the client.

A periodic transmission strategy using a sequence of joint beamforming gain and artificial noise pairs is developed in [118]. This sequential transmission strategy enables communications to a client while ensuring that no receiver in a known sector can decrease its uncertainty on the information bits by eavesdropping.

A related study considers groups of distributed beamformers, with two agents per group [119]. A two-antenna element solution provides beam shapes that are broad in angle and are favorable for shaping artificial noise transmission when an eavesdropper location is known to be within a relatively large angular sector. Fig. 7 illustrates a scenario with two groups, where each group has two agents. The rotation angles for each group (denoted $\theta_{G,1}, \theta_{G,2}$ in the figure) and the antenna phase components are jointly optimized to transmit artificial noise while null-forming to the client. The rotation of each group helps to orient a broad artificial noise beam over a desired jamming region, while also nullforming to the client. The result is to maximize the radiated artificial noise energy over an angular sector containing the eavesdropper while placing a null towards the client. Simulations demonstrate artificial noise radiation patterns at low frequency (40 MHz) [119].

A network coverage problem with distributed beamforming under a Ginibre point process (GPP) model on the random spatial distribution of networked nodes is considered in [120]. The GPP is a point process model with tunable repulsion, used to model the dispersion of agents. The analysis also incorporates phase offset errors due to a lack of perfect carrier synchronization among agents. Analytical expressions accurately predict the coverage probabilities as a function of the agent dispersion and in the presence of the phase offset errors, for both transmitter selection and coherent beamforming strategies.

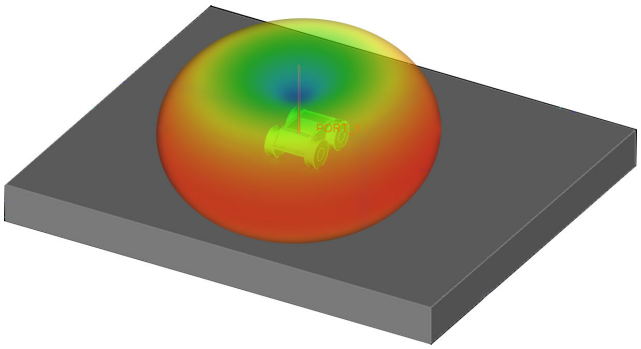

FIGURE 8. Electromagnetic radiation pattern of a single low-VHF electrically small antenna mounted on a ground robot; from [125]. ©2019 IEEE.

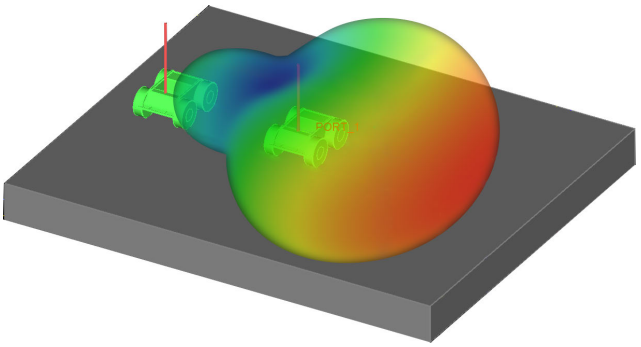

FIGURE 9. Parasitic two-element antenna array radiation pattern. A second robot carries a passive antenna that mutually couples with the active antenna of the robot in Fig. 8; from [125]. ©2019 IEEE.

IX. PARASITIC AND COMPACT ARRAYS

When antenna elements are closely spaced with respect to the wavelength then electromagnetic coupling becomes significant. In this section we review two recently developed approaches that exploit this coupling in low frequency arrays. Parasitic (passive) antenna elements can be placed to alter the beampattern and gain, described in section IX-A. As antenna element spacing becomes a small fraction of the wavelength then the coupling increases. This coupling can be exploited in a compact array with an appropriately designed electrical coupling network, described in section IX-B.

A. PARASITIC ARRAYS

A parasitic array is composed of one or more active antenna elements connected to a radio and one or more passive antenna elements that serve as passive radiators and are not directly connected to the active elements [121]. The parasitic elements passively couple with the active elements and affect the beamshape. Electrically steerable parasitic arrays are possible, e.g., in an end-fire array configuration [122]. A constellation of coupled antenna elements may be selectively switched from passive to active to preferentially radiate towards a specific sector at a desired power level [123], [124].

At low frequencies, these arrays tend to be large, with element spacing on the order of $\lambda/2$. However, parasitic arrays offer a low complexity approach for distributed arrays, e.g., by placing the passive antenna elements on multiple robotic platforms. When implemented on ground robots they can collaborate to create an array of a desired size and directionality and their motion can reorient the preferred radition of the array. An appealing approach is based on the classic Yagi-Uda array with a single active antenna on a robotic platform and parasitic elements on nearby robots.

The idea is illustrated in Figures 8 and 9. Figure 8 shows the radiation pattern for a single omnidirectional antenna on a ground robot (the robot's antenna radiates in a nearly omni-directional pattern except along the vertical antenna axis), and Figure 9 shows the radiation pattern when a second robot with a parasitic element is introduced. These figures are derived from a full wave finite-difference time-domain (FDTD) simulation. Unlike a classic Yagi-Uda free-space design, the coupling is affected by the ground medium and this affects the optimal antenna spacing. The parasitic element, that is functioning as a reflector, is placed to the upper left of the single transmitting robot. By forming a parasitic array, more power is radiated to the lower right as shown in Fig. 9.

Insight can be gained from analysis of the two-element case with vertically oriented half-wave dipoles, showing how the beampattern is a function of the antenna spacing and their orientation [126], [127]. Intuitively, the reflection from the passive element phase-aligns with the active element transmission to provide gain along the two-antenna axis. Note that the parasitic array has the same beampattern on transmit and receive. More active and passive elements can be included. For the robotics application combining one active and multiple passive antennas is appealing, requiring only one robot to actively transmit.

Low frequency robotic experiments have demonstrated parasitic arrays that maintain their radiation pattern gain in both line-of-sight and non-line of sight scenarios [128], meaning that they can extend communication range in complex urban environments. Experiments and simulations show how these arrays can increase communication range and beam confinement, for example, by aligning more robots with parasitic antennas to form larger arrays. In [129] a model for multi-element robotic parasitic arrays is applied to the problem of network connectivity, and this is used to allocate parasitic elements (carried by robots) throughout the network to increase the overall network connectivity as measured by the Fiedler value of a connectivity graph.

B. COMPACT COUPLED ARRAYS

The distributed and parasitic arrays discussed in Sections VIII and IX-A require control of the relative positions of multiple antennas and/or the phases of the respective transmit signals. Distributed arrays additionally require time and frequency synchronization of multiple radios. Integrating an antenna array on a single platform eases the positioning and

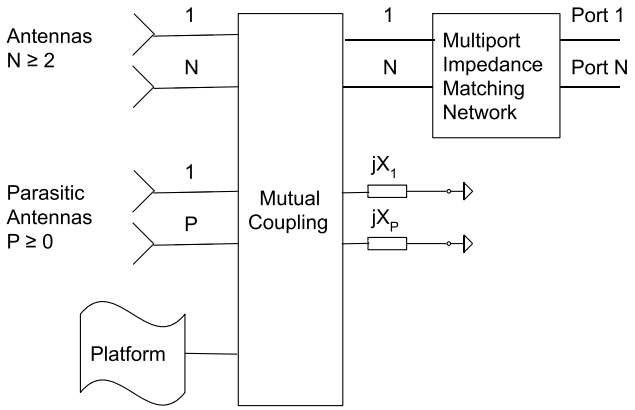

FIGURE 10. Elements of a compact antenna array system, with electromagnetic coupling due to small inter-element spacing relative to the operating low frequency wavelength. Parasitic antennas are optional; if present they are terminated with a reactive impedance or short circuit.

synchronization requirements but brings different challenges and opportunities. For example, at 40 MHz ($\lambda = 7.5$ m) the platform dimensions may be much smaller than λ so the array will be electrically small. Inter-element spacing much less than $\lambda/2$ results in strong mutual coupling that must be accounted for. The general elements of a compact (not necessarily linearly spaced) array on a platform are illustrated in Figure 10. The system contains $N \geq 2$ antennas that are mutually coupled with each other as well as the platform. This may include P passive parasitic antennas that are terminated with a short circuit or reactive impedance, and these will also couple with nearby antennas and the platform. Ideally, the antennas and their placement on the platform are designed (e.g., with computational electromagnetics software) to achieve desirable radiation characteristics at the operating frequency, but strong mutual coupling between the antennas will persist due to the small spacing. In the works described below, the platform effects are ignored and the focus is on compact arrays.

When the compact array is used as a receiver the ports 1 to N in Figure 10 feed a multichannel radio, typically with $R = 50\ \Omega$ input impedance per channel. When used for transmission the N ports are fed by signal generators, typically with $R = 50\ \Omega$ internal impedance. For both transmit and receive a multiport impedance matching network is required to eliminate reflections between the terminals of the active antennas and the generators or receivers [130], [131], [132], [133]. If the network matches the impedance of the active antennas, including the mutual coupling, then all of the available power from the antennas is delivered to the receiver(s), and all of the available power from the generators is radiated by the antennas (resistive losses in the matching network and antennas are discussed below). Without the matching network, on receive some of the available power is reradiated (scattered) from the antennas rather than being delivered to the receivers, and on transmit some of the generated power is reflected back and dissipated in the generators rather than being radiated by the antennas. Note this implies the impedance matching must be performed in the analog domain. The power losses from reflections cannot be reversed by digital processing of the received signals or modification of the complex beamforming weights applied to the signal generators. The matching network is especially important for electrically small compact arrays where reflections may be large in some modes [134].

Multiport impedance matching networks are also referred to as external coupling networks (ECNs) [135], decoupling and matching networks (DMNs) [134], [136], and other descriptors [133], [137]. The term ECN is used in this section for simplicity and we consider ECNs that are linear, passive, lossless, and reciprocal. ECNs are implemented with lumped circuit components (inductors or capacitors), distributed reactive components (transmission lines), parasitic antennas, or a combination of these components [133], [136]. Lumped elements may provide more compact ECNs at low frequency than transmission lines. Note that various designs may yield signals at ports 1 to N that differ by a linear transformation, although the general objective is multiport impedance matching at the operating frequency. Also, in some high performance communications applications a noise matching objective for the network design may be more appropriate [130], [138]; here we focus on impedance matching.

Parasitic antennas are indicated as optional elements in Figure 10, and they have been shown to improve compact array systems by increasing the effective radiation resistance of the active antennas [139], increasing the system bandwidth [139], [140], or simplifying the matching network by decoupling the active antennas [136], [140], [141]. Therefore the parasitic antennas, if included, may be considered as part of the impedance matching subsystem. A small one-port antenna at low-VHF with closely-spaced parasitic antennas has been designed and fabricated for small robotic platforms [142]. However, the general application of parasitics in low frequency compact array systems on small platforms has not been fully investigated.

1) TWO-ELEMENT COMPACT ARRAY

As an illustration of beamforming and direction finding, consider an $N = 2$ element compact array with half-wavelength dipole antennas at 40 MHz and spacing d between the elements. This example illustrates the effects for two values of d; for simplicity in developing the theory and simulations we use dipoles although they are long, and much smaller antenna elements can be used. We show beamforming power gain and angle of arrival estimation performance in Figure 11. Here azimuth angle θ is defined relative to 0° at broadside and ±90° at endfire.

Figure 11 shows numerical results for antenna spacings $d/\lambda = 0.05$ (compact array) and $d/\lambda = 0.4$. In each case we incorporate an ECN that is optimal for the specific choice of d/λ. The top panel shows the maximum relative power gain

of the array for each d, defined as the best achievable gain at that angle relative to a single antenna. The larger antenna spacing has little mutual coupling, and the maximum relative gain is roughly equal to 2 ($\approx$ 3 dB) for any angle (red curve). The compact array, with significant mutual coupling, has gain that varies with angle (curve). At broadside the gain is close to 1, the same as that achieved with a single antenna, whereas at endfire the gain is 3.4 (5.3 dB). The compact array gain is referred to as supergain or superdirectivity, because the gain is beyond that achieved with two uncoupled antennas, and is fundamental to the compact array utility. Assuming lossless antennas and optimal ECN, then on transmit this relative gain corresponds to the maximum directivity of the array as a function of angle normalized by the directivity of a half-wavelength antenna. On receive the relative gain can be interpreted as the maximum effective area of the array in each direction normalized by the effective area of one antenna [143].

The black line in Figure 11 (top panel) shows the gain of the compact array relative to one antenna when the beam is fixed and steered to $\theta = 90°$. The same directional gain is achieved for both transmitting and receiving. The maximum gain is 3.4 (5.3 dB) at the steering angle $\theta = 90°$, with a null at $\theta = -25°$.

The bottom panel in Figure 11 shows direction finding performance characterized by the theoretical Cramer-Rao lower bound (CRB) on the variance of estimating the angle of arrival (AOA) parameter θ with noisy measurements [143], [144]. The bound accounts for the presence of an analog ECN, and is achievable by sampling the ECN outputs and applying a maximum likelihood estimator. For this example the received signal to noise ratio is set to 20 dB. The two curves show the bound for each value of d. It is well known that a two-element array yields the best angle estimation performance (lowest theoretical CRB) at broadside, and the estimation performance degrades as the source angle approaches endfire, resulting in the u-shape curve. It is also well known that, as d becomes smaller then the CRB will shift upward (the AOA estimation performance will become much worse). However, when the compact array with $d/\lambda = 0.05$ is augmented with the optimal ECN, as shown in the Figure, then the CRB remains close to the performance with the larger $d/\lambda = 0.4$ spacing. Remarkably, the analog ECN preserves angle information by accounting for the mutual coupling induced by the small spacing, and the ECN output can be sampled and processed to obtain AOA accuracy that is otherwise significantly degraded without the ECN.

Taken together, the results show that with the two-element compact array angle estimation is most accurate at broadside, whereas beamforming has maximum gain at endfire. These could both be exploited, e.g., on a rotating robotic platform. Alternatively, a compact symmetric three-element triangular array with spacing $d/\lambda = 0.05$ has gain 3.4 in all directions [145], and it can be shown that when an optimal ECN is used this array has uniform CRB in all directions. Thus, a three-element triangular design is angle independent

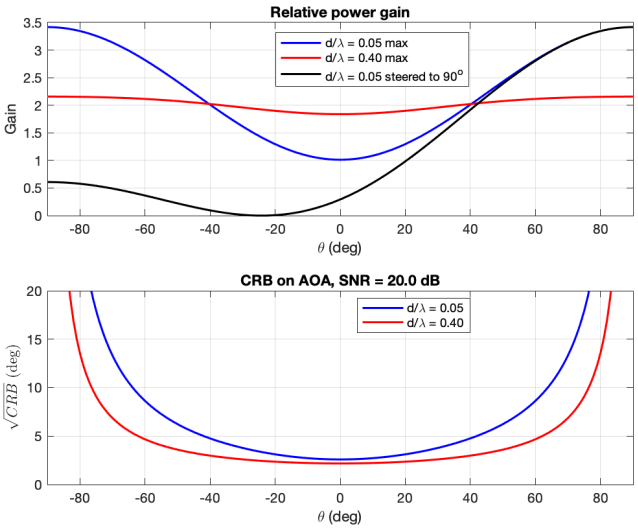

FIGURE 11. Two-element antenna example with spacing d and wavelength λ, from [143]. Top: array gain versus angle of arrival, relative to a single antenna. The compact array exhibits supergain near endfire (±90°). Bottom: theoretical Cramer-Rao lower bound on angle of arrival estimation. With the optimal analog coupling network the compact array preserves the angle information despite the very small spacing.

for both beamforming and direction finding, and has a compact size relative to the wavelength.

As noted earlier, it is important to consider resistive losses and system bandwidth that have been ignored in the two-element compact array example above. The impedance matching with an ECN is achieved at the design frequency, but the match diminishes with increasing bandwidth. The Chu-Wheeler limit for passive antennas (discussed in Section VI and [88]) implies that a compact array must have a smaller fractional bandwidth-radiation efficiency product than an array composed of the same antennas with larger spacing [146], [147]. Radiation efficiency refers to resistive power loss in the antennas, so maximizing compact array efficiency comes at the cost of reduced bandwidth. Compact arrays are inherently less efficient in some modes that have small radiation resistance [134], so the realizable superdirectivity/supergain is reduced. The ECN for these modes may also incur greater resistive losses that further degrade the overall system efficiency.

Compact, superdirective antenna arrays have been extensively studied for more than 80 years [146], [147], [148] with significant recent interest for direction finding [144], [149], beamforming [150], [151], [152], MIMO communication [153], [154], [155], [156], and wireless power transfer [148]. Some investigations are pessimistic and report that losses negate the superdirectivity [134], [153], [154], while others are more promising with acceptable measured performance in fabricated systems [135], [148], [151], [152], [156], [157], [158], [159], [160], [161]. Compact array systems are feasible in practice as long as the number of antennas is not too large and the spacing is not too small [146], [147], [161], so careful system design is essential. With reference to Figure 11, even if the losses with smaller spacing

reduce the realized gain to the same level as the larger spacing (a gain of 3 dB), the ability to achieve this performance at low frequency with a compact array is important for small platform applications such as robotics.

Biomimetic antenna arrays (BMAAs) are a class of compact array systems that have been investigated during the past decade primarily for direction finding [135], [144], [145], and also for MIMO communications [156]. The ECN in BMAAs consists of lumped circuit elements or transmission lines and measurements from several fabricated systems are reported to agree reasonably well with simulations assuming lossless antennas and an ECN. A notable first step in mounting a low frequency compact array on a robot operating at 40 MHz is described in [162]. An array with two electrically small antennas was designed with the platform as part of the radiating structure. The system was fabricated and experimentally tested without an ECN. Simulations with an ECN developed for BMAAs show improved impedance matching and direction finding performance.

The distributed and parasitic arrays discussed in Sections VIII and IX-A share the same elements as in Figure 11, so it is instructive to compare them to a compact array. In a distributed array each antenna is independently impedance matched to the receiver or generator, and multiport impedance matching is not possible. Therefore in a distributed array the antennas should be positioned so that mutual coupling is minimized, otherwise power loss will occur from reflections due to the uncompensated coupling. In a parasitic array with $N = 1$ active antenna and $P \geq 1$ passive antennas as described in Section IX-A, the spacing is much larger than a compact array and is carefully tuned to achieve increased spatial gain [125]. Also, compared with compact arrays, the bandwidth of distributed and parasitic arrays is generally greater because the total array size is typically much larger and they are not operating in an electrically small regime.

In a multi-agent setting, mounting compact low frequency arrays on each agent leads to improved sensing and networking capabilities relative to an omnidirectional antenna on each agent. Individual agents can perform direction finding, and together agents can cooperatively transmit and receive for increased network throughput and interference rejection. Combining multiple compact arrays into a larger distributed array is also an interesting research direction.

General design techniques for electrically small antennas [88] are also applicable to compact arrays, including multiport active (non-Foster) impedance matching for increased bandwidth [163], frequency-tunable ECNs [164], and metamaterials [165], [166]. These designs could be coupled with platforms and ECNs for enhanced performance.

X. MULTI-USER CODING & EXPERIMENTATION FOR AUTONOMOUS AGENT NETWORKING

The use of low frequency for ad hoc multi-user networking in complex environments has motivated recent advances in multi-user direct sequence code division multi-access (DS-CDMA). In this section we describe recent enhanced variations of multi-user coding schemes that have been investigated to support CDMA with relaxed synchronization, frequency offset, and orthogonality requirements. This approach to multi-user networking is appealing for mobile multi-agent autonomous system networking and doesn't require fixed infrastructure such as a centralized basestation. The proposed strategies are of general interest, and their impact is especially significant when enabling low frequency ad hoc networking in extreme propagation environments. These signal designs, combined with low frequency operation, enable effective near-orthogonal ad hoc networking. Their use in non-orthogonal networks is considered in Section XI.

A. QUASI-SYNCHRONOUS MULTI-CARRIER CDMA

In CDMA, the choice of the spreading code determines many relevant properties of the resulting communications system [167], [168], [169]. However, classical spreading codes (e.g., Gold codes) have non-zero cross-correlations [169], [169], [170], so imperfect synchronization leads to multi-access interference (MAI), and power mismatch leads to the near-far problem. The near-far problem is a vexing challenge for highly flexible autonomous networks that aim at high mobility and on-the-fly routing decisions, while maintaining reliable and efficient connectivity. So, the design of codes that reduce the synchronization requirements and manage cross-correlation interference is important.

The synchronization requirements can be reduced with the use of loosely synchronous (LS) codes [171], [172] to enable quasi-synchronous (QS) multicarrier (MC) DS-CDMA [173], [174], [175], [176], [177], [178], [179], [180], [181], [182], [183]. This has two principal advantages. First, these codes are characterized by a zero cross-correlation zone (ZCZ) [171], [172], a measure of the extent to which two nodes can be unsynchronized in time but still retain perfect code orthogonality. Loosening the time synchronization requirement reduces receiver complexity and network coordination costs, and perfect orthogonality eliminates, in principle, MAI and thus the need for power control. Second, the use of multiple carriers enables extension of the time duration of the ZCZ, thereby further relaxing the time synchronization requirement in proportion to the number of subcarriers.

However, frequency offset between nodes causes a loss of code orthogonality and the problem becomes worse when using multiple carriers in MC-CDMA [182], [183], [184]. In practice time and frequency may be controlled by a common clock, so that a node that is coarsely time synchronized will also be coarsely frequency synchronized. The presence of frequency offset in LS codes is an important and relatively less studied design consideration.

A well-known and nearly optimal (in the sense of the number of spreading codes generated) construction technique for a ZCZ code family is based on the concatenation of several

constituent complementary sequences and their mates, each of which is multiplied by the entries of a Hadamard matrix. This procedure gives rise to a large number of ZCZ code families, with each family parameterized by a choice of the complementary sequence pair and Hadamard matrix used. While the resulting code families have identical properties in time (e.g., the existence of a ZCZ over which ideal auto-correlation and cross-correlation properties hold), each has different performance with respect to frequency offset and some families are more sensitive to frequency-offset induced orthogonality loss than others.

Motivated by low frequency CDMA, a comprehensive numerical search was conducted over a large collection of ZCZ code families that examined the best- and worst-achievable performance in terms of frequency-offset induced orthogonality loss. These codes were studied for QS multi-user networking applications at low VHF, including simulations and experiments on software-defined radios that have non-trivial frequency offsets [185], [186].

B. QS-MC-CDMA INDOOR/OUTDOOR EXPERIMENTS WITH LOOSELY SYNCHRONIZED CODES

Adopting multiple carriers extends the symbol time and so it also extends the time duration of a ZCZ, thereby relaxing the overall CDMA time synchronization requirement for mobile autonomous agents. However, MC-CDMA is more susceptible to frequency synchronization errors at the receiver than a single-carrier system. The time/frequency synchronization tradeoff for multi-carrier networks employing ZCZ codes is studied experimentally in [185], through software defined radio (SDR) experiments at low frequency, with low power transmission in densely cluttered environments. This work highlights the promise of QS-MC-CDMA signaling to enable low frequency multi-user communications. Experiments showed excellent interference rejection properties in scenarios involving i) coarse time and frequency synchronization, ii) near-far scenarios, and iii) non-integer chip delays. Longer codes are less susceptible to timing uncertainty due to a larger ZCZ, while they are more susceptible to frequency offset uncertainty since the accumulated phase will degrade the receiver detection performance and LS code multi-access interference suppression. Low VHF experiments demonstrated that varying the ZCZ size and code length enables a flexible tradeoff between time and frequency synchronization requirements.

QS-DS-CDMA SDR experiments studied ZCZ performance in and around a large five story building, including constellations up to 256-QAM [186]. The SDR testbed in Figure 12 enabled software control of the signals and system parameters, and cabling was used to vary the physical spacing of the two transmit antennas. Low VHF short ($\lambda/6$) dipole antennas were used with center frequency of 40 MHz and 3 dB impedance bandwith of 3 MHz. Various levels of imperfections were under software control including synchronization, frequency offset and power mismatch between users.

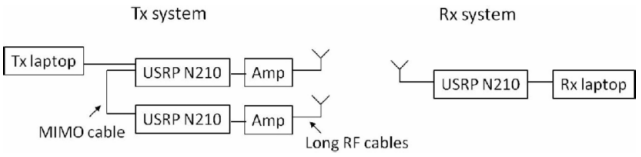

FIGURE 12. ZCZ experimental testbed configuration, with two transmit and one receive USRP SDR. The Tx USRPs are wired to enable programmable offsets, and the Tx antennas are spread using lengthy RF cables. From [186]. ©2017 IEEE.

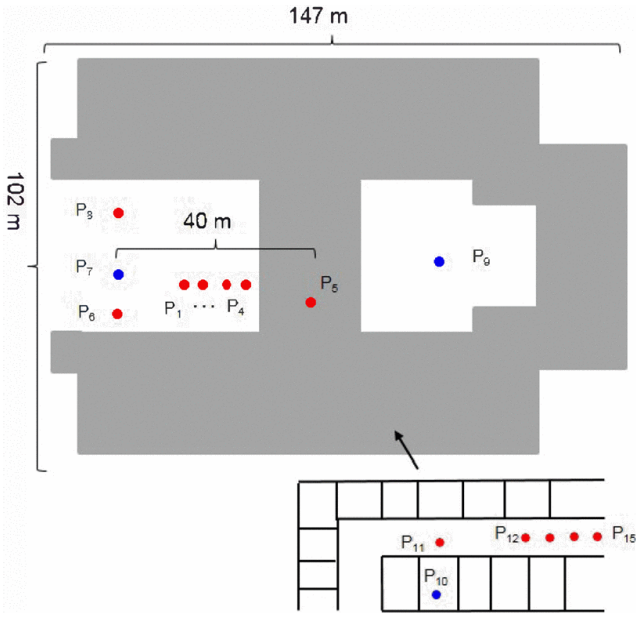

FIGURE 13. ZCZ experimental measurements were carried out in and around a large, highly cluttered five story building with extensive metal partitions and reinforcements. The building is shown in gray, with outdoors and courtyard show in white. NLOS indoor/outdoor and through-building cases were studied. From [186]. ©2017 IEEE.

Figure 13 depicts the building used for experiments and in- and thru-building test points. Figure 14 shows a through-building SINR for one of two co-channel users. The results demonstrate low MAI with inter-user time offset within the ZCZ, and limited degradation outside the ZCZ. Figure 15 shows experimental 256-QAM constellation diagrams for an in-building NLOS experiment, plotted for varying time-delay offsets between the two users. A simple correlator receiver was used, matched to the user of interest. Increasing MAI is evident as the inter-user time delay increases beyond the ZCZ.

The effect of frequency offset was also studied experimentally (see Figure 16), and shown to have relatively minor impact for the scenarios considered with inter-user frequency offsets of 10's of Hz.

XI. NON-ORTHOGONAL MULTI-AGENT NETWORKING

The multi-user codes described in Section X are not only well suited for low frequency CDMA applications, but also for scalable non-orthogonal ad hoc networking. Increasing the number of agents in an ad hoc CDMA network leads to difficulties in orthogonal code allocation and network

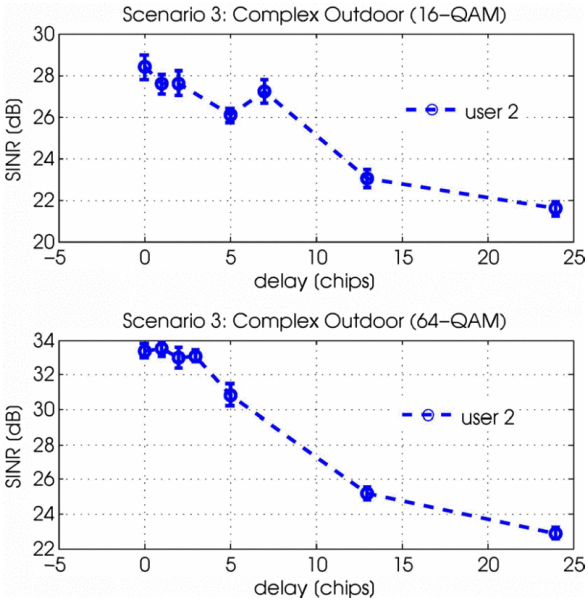

FIGURE 14. ZCZ SDR experimental result: The SINR measured for the user of interest (transmitter 2) vs delay in chips (6.4μ secs) for 16-QAM and 64-QAM. Transmitter 2 and transmitter 1 were located at P6 and P8, respectively, and the receiver is positioned at P9 (see Figure 13). From [186]. ©2017 IEEE.

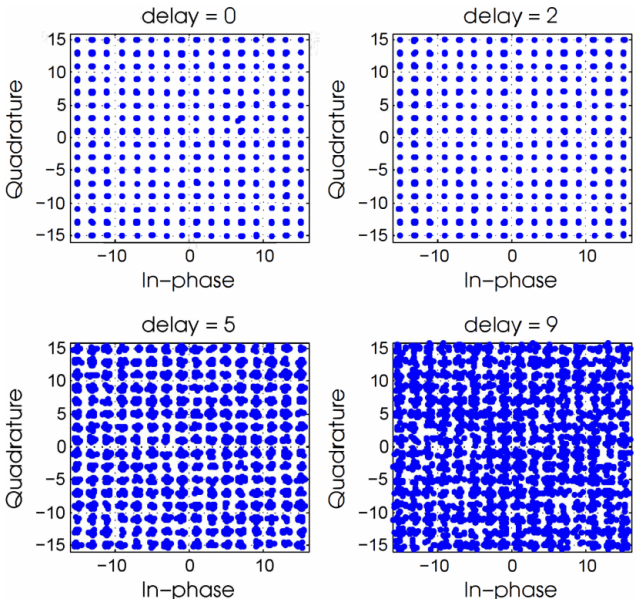

FIGURE 15. ZCZ experiment: The constellation diagram for a 256-QAM versus inter-user delays within and outside of the ZCZ. The experiment is carried out in a scenario where transmitter 2 and user 1 are located at P15 and P11, respectively (see Figure 13). The constellations are much tighter for delays within the ZCZ compared to those outside ZCZ since interference rejection is very high when the relative delays are within the ZCZ. The computed SINR for delays within ZCZ is 51 dB. At delay 5 and 9 chips, the SINRs are 31 and 27 dB, respectively. From [186]. ©2017 IEEE.

coordination for synchronization and interference management. The difficulty is exacerbated with mobile autonomous agents and may lead to a coordination overhead that impedes fast and flexible network deployment for required communication rates. Removing the requirement of orthogonality

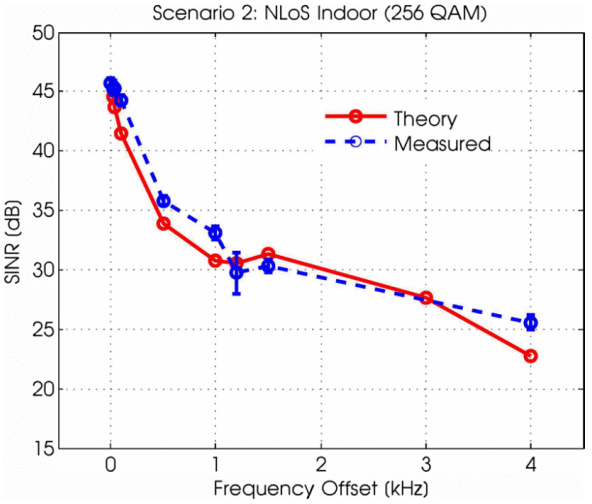

FIGURE 16. ZCZ experiment: The measured and theoretical SINR for the user of interest varies within 4 dB for frequency offsets up to 100 Hz, while continuing to degrade for higher frequency offsets. The experimental scenario is the same as in Figure 15. From [186]. ©2017 IEEE.

leads to the study of low frequency non-orthogonal multiple access (NOMA) networking, the topic of this section.

A. NON-ORTHOGONAL AUTONOMOUS NETWORKING WITH WBE ACHIEVING CODES

As the number of agents in a CDMA network rises it can become overloaded, so that code orthogonality is not achievable even under ideal synchronized conditions. When using multi-carrier modulation, low frequency channels may exhibit low variation in the per-carrier phase response, and this can be exploited to relax the inter-user time synchrony requirements of an overloaded (i.e., non-orthogonal) MC-CDMA network.

Theorem 1 in [187] provides a bound on code cross-correlation that is a function of the number of users, sequence length, the maximum inter-user delay and the maximum per-carrier channel response variation. It is shown that any Welch-Bound Equality (WBE) achieving code (e.g., see [188], [189]) will obey the bound [187]. This enables a tradeoff analysis between user overload in non-orthogonal multiple access (NOMA, e.g., see [190], [191], [192]), inter-user delay, phase variation, user activity and the required signal-to-interference (SIR) decoding threshold, for a given MC-CDMA network topology. For low-VHF and other propagation channels where the variation in the phase and amplitude response can be neglected, the relationship between maximum inter-user delay and the required SIR performance threshold is characterized, and it is demonstrated that by searching over large families of Walsh-Hadamard codes, one can improve the L_1 interference norm significantly [187]. FDTD-based low-VHF numerical propagation modeling through buildings provides evidence that the amplitude and phase channel-variation can be very limited, so that appropriate code choice can relax synchronization requirements.

B. SCALABLE SPORADIC NON-ORTHOGONAL MAC [193]

Supporting networks with a large number of nodes in infrastructure-poor and complex propagation environments is an important challenge for multi-agent autonomous systems applications. A major problem when using classical approaches, such as code division multiple access (CDMA), is maintaining inter-link coordination while mitigating multi-user interference (MUI). Sporadic channel access allows one to capitalize on random code reuse and enable efficient non-orthogonal medium access [190], [191], [192]. This approach is appealing for low frequency operation with superior penetration, reduced multipath, and increased channel coherence time for near-ground communications and in complex environments [83], [185], [186]. The advent of miniature low frequency antennas enables practical device to device (D2D) applications, including small autonomous agents with limited power budget [194], [195], [196].

In [193], the authors develop a scalable sporadic MAC for low-frequency ad-hoc networking, incorporating shift-orthogonal coding and weak network synchronization (see Section X). Various levels of code reuse, synchronization and coordination are considered. Of particular interest is a purely random (uncoordinated) spreading code assignment. The results illustrate good performance of a scalable medium access scheme. The study uses accurate full-wave electromagnetic simulations based on high fidelity RF propagation modeling of a low-VHF 3-D building model, as shown in Figure 17. This channel modeling approach captures signal variation in terms of both amplitude and phase within a desired bandwidth (see Section IV). This environment provides a backdrop for realistic analysis of large-scale sparse D2D networking simulations.

The study employs a quasi-synchronous code-division multiple-access scheme that enables significantly reduced synchronization requirements, and together with the sporadicity in network activity mitigates the inter-link interference and the near-far problem. The code assignment and reuse strategies allow the network to scale while maintaining acceptable performance. An instantiation of the proposed approach with low power (10s of mWs), coarse time synchronization requirement (20 μsecs), and sporadic communications among users performs well. The network traffic was simulated from the perspective of a receiver trying to decode a randomly selected user of interest, where other users are treated as interference. Medium access was based on a slotted transmission approach with CDMA multiplexing.

Simulation results in the building environment of Figure 17 are shown in Figures 18 and 19. Figure 18 (top) shows packet error rate versus probability of transmission for different reuse factor ρ. Figure 18 (bottom) illustrates three different levels of synchrony, where a loosely synchronous MAC maintains good performance within the zero-correlation zone (“Within Z”). Figure 19 considers code reuse protocols, illustrating how random reuse and round robin schemes perform well with maximum delays within the zero-correlation zone of the code family. The results suggest that code reuse,

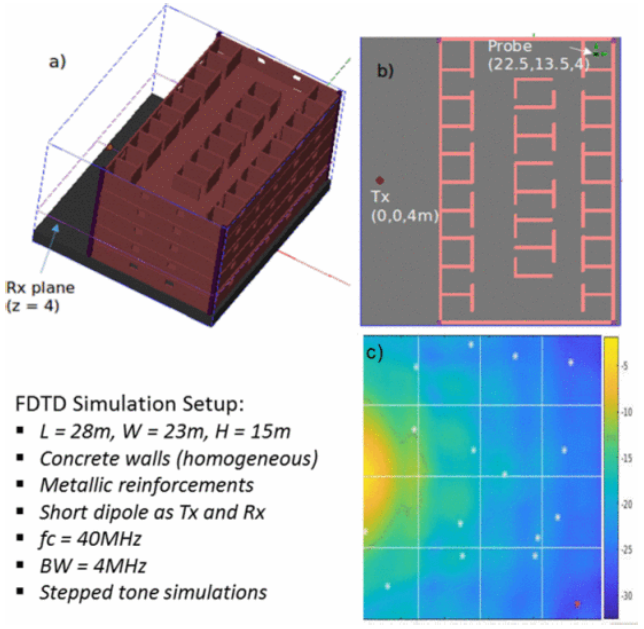

FIGURE 17. Building model for low-VHF sporadic MAC study, from [193], ©2018 IEEE. (a) Five story 3-D building model, (b) building single floor, top view. In (b), the ceiling and floors are not shown for ease of visualization. (c) Example of signal coverage with nodes randomly placed within grid of sub-regions.

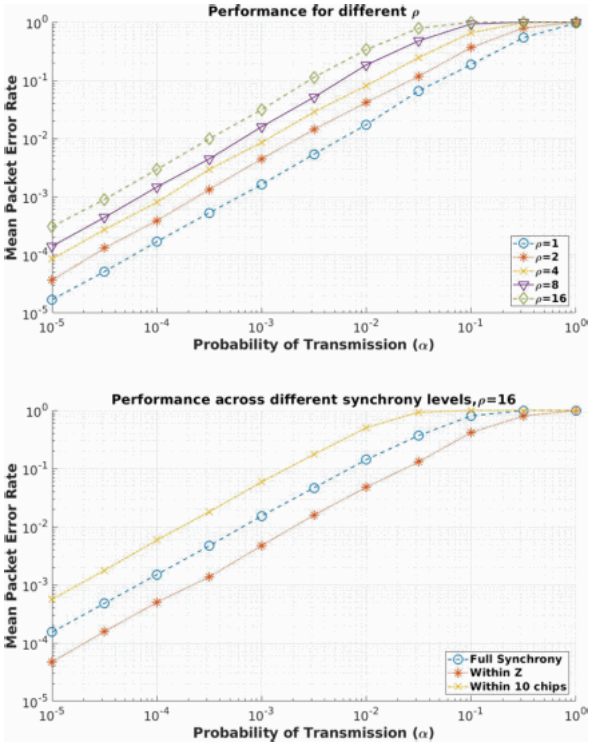

FIGURE 18. Low-VHF sporadic MAC study, from [193]. Packet error rate vs transmission probability (a) for different reuse factors ρ, and (b) three levels of synchrony. Loosely synchronous CDMA within the zero-correlation zone performs well.

even with random reuse strategies, can augment the pool of available CDMA codes in sporadic and loosely synchronous

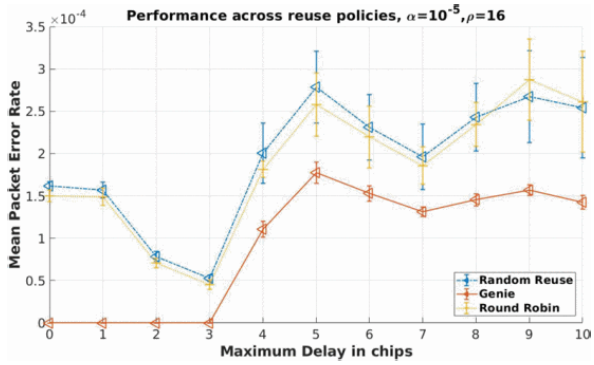

FIGURE 19. a) Rate of packet error curve vs probability of transmission for different values of communication sporadicity ρ, using the results from FDTD simulation. The synchrony level was fixed at $\tau = 10$ chips; channel effects included. b) Rate of packet error vs probability of transmission for different levels of synchrony at $\rho = 16$. From [193]. ©2018 IEEE.

D2D low frequency networking environments with tolerable effects on packet error rate.

XII. CONCLUSION

Multi-agent autonomous systems are rapidly maturing and being applied in a variety of important cases, and reliable networking is key to their collaborative success. However, multi-robot wireless networking is very challenging, especially in complex environments. These challenges require autonomous systems to adapt to changing and difficult conditions with uncertain networking [5].

We have described many recent combined advances on the use of low frequency in support of mobile autonomous systems, especially collaborative autonomy in dense urban and indoor/outdoor scenarios. Topics included low frequency propagation modeling, networking, miniature sub-wavelength antennas and electromagnetics for mutually coupled antenna arrays, geolocation techniques, multi-antenna array distributed beamforming, and mobile collaborative processing. These advances generally exploit the low frequency propagation and tightly couple with autonomous networking and distributed processing goals.

A. CHALLENGES AND LIMITATIONS

The use of low frequency in a decentralized setting requires careful attention to multi-access and other forms of co-channel interference. The enhanced propagation in complex environments is very desirable, yet also can lead to more mutual interference between users when there is no centralized network management to maintain user orthogonality. The advances in multi-user coding and channel access described in Sections X and XI present some important techniques that address the multi-access problem. Using adaptive power control and other cognitive networking techniques would likely be highly beneficial, including co-channel interference rejection techniques. The propagation can change significantly between indoor or outdoor and as elevation increases, underlining the need for power control mechanisms that adapt to mobility. Low frequency communications standards often require very narrowband channels, and minimizing neighboring channel interference is also important to consider.

As is common for wireless radio, propagation channel modeling depends on the environment. For low frequency, the Rician model appears to be reasonably general. However, modeling the penetration into buildings may require numerical studies and experiments; see the summary review in Section IV-F.

Employing low frequency on small platforms leads to the need for electrically small antennas, and small arrays. Electrically small antennas have been extensively studied, and Section VI provides an overview and links to the literature. Electromagnetic coupling and platform integration are important issues that complicate the use of low frequency for robotics, as dicussed in Section VI. The electromagnetic coupling between closely spaced antenna elements is a classic problem, and recent research on exploiting the coupling in very small baseline arrays described in Section IX presents new techniques that appear promising for low frequency applications. More research and experiments are needed to mature these ideas and put these into practice.

B. OPPORTUNITIES

The use of low frequency necessarily comes with signal bandwidth limitations. Nevertheless, reliable low bandwidth networking can provide a distributed control backbone, support geolocation and collaborative reasoning, and provide a human-machine interface from a distance. As autonomous systems science progresses, it is likely that communications requirements will be reduced as individual agents become more capable, so that persistent low bandwidth connectivity may be sufficient for many distributed control scenarios.

Low frequency ad hoc networking can support adaptive and opportunistic collaborative autonomy. For many applications, advanced forms of reasoning using artificial intelligence are leading to highly compressed and specific information representations that may be shared intermittently, without the need for persistent high bandwidth communications. Advances in multi-user networking and cognitive radio have been shown to be effective for low frequency channels, and these methods generally have low computational requirements that benefit from the propagation channels and the narrow signal bandwidths. Coupled with intelligent group mobility, these techniques offer new means for supporting collaborative autonomous systems that will be used for critical applications such as disaster response and public safety.

Commercial wireless systems are progressing to interoperability and internetworking, such as the combination of cellular, WiFi, and Bluetooth in mobile devices. Public safety networks are also progressing to interoperability with cellular systems (see Section III). In addition, optical and mmWave communications are rapidly maturing and mmWave is being studied extensively for potential integration into 6G cellular

networks. These trends highlight the benefit of multi-radio integration, combining the strengths of each to result in a significantly enhanced overall network for various applications.

Low frequency, with efficient small antennas and software defined cognitive functions, can complement existing medium and higher frequency technologies [197]. A **multi-radio system solution including low, medium, and high frequency** is appealing for mobile autonomous agents that combines:

- **High-frequency high-bandwith,** such as optical and mmWave, provide very high bandwidth links and use spatial beamsteering for directionality. Agents may move to achieve line-of-sight links as desired or exploit them opportunistically.
- **Medium-frequency medium-bandwidth,** such as cellular and WiFi, provide MHz of bandwidth when channel conditions are favorable. This may be through conventional cellular and WiFi infrastructure, or ad hoc connectivity.
- **Low-frequency low-bandwidth,** as described in this paper, could provide a low bandwidth ad hoc backbone that persists and operates in complex environments.

Several experimental studies described in this article used autonomous mobility and sampling to **rapidly and efficiently collect large data sets**. Exploration can be intelligently guided by maximizing an information-based criteria [198]. This enables multiple agents to collaborate in a variety of ways, including real-time communications network characterization and collaborative localization. Autonomous data collection can be used for learning an environment, combining different frequencies for communications, finding a radio source (such as for search and rescue), using mobility to ensure a desired network topology, and in a variety of other ways to support multi-agent autonomy.

Several promising areas have not yet been fully explored for low frequency application, including the following.

- **Sensing-based dynamic spectrum access** (e.g., see [199]), coupled with multi-user coding and non-orthogonal multi-access (NOMA), could be an effective method for adaptation without a high degree of synchronization. Many cognitive methods are now available for inferring spectrum occupancy in a broad time-frequency-space perspective [49].
- **Full duplex** communications appear very promising for narrow band low frequency use. Here, three critical parameters are relaxed in comparison to implementing full duplex at higher frequencies: power, bandwidth, and delay spread [200], [201], [202]. When increased, all three of these stress full duplex solutions, and the relatively low values for all of them in short range low frequency applications simplifies the technology challenges for low frequency adoption.
- **Learning-based channel modeling and prediction** techniques could be beneficial and provide environment adaptation, perhaps learning from both numerical models and physical measurements. The full-wave numerical methods are computationally expensive, and this motivates learners that approximate or extrapolate from examples to a broader range of applicability and less dependence on specific environments.

The **merging of cognitive networking and autonomous systems** will support increasingly sophisticated autonomous behaviors in challenging environments. As the modern tools and techniques continue to emerge and mature, the potential for new applications and use of low frequency communications will be further revealed.

REFERENCES

[1] H. Chen, P. Hovareshti, and J. S. Baras, "Communication network challenges for collaborative vehicles," in *Proc. Conf. Rec. 45th Asilomar Conf. Signals, Syst. Comput. (ASILOMAR)*, Nov. 2011, pp. 1472–1476.
[2] Y. Wu, X. Ren, H. Zhou, Y. Wang, and X. Yi, "A survey on multi-robot coordination in electromagnetic adversarial environment: Challenges and techniques," *IEEE Access*, vol. 8, pp. 53484–53497, 2020.
[3] J. Gielis, A. Shankar, and A. Prorok, "A critical review of communications in multi-robot systems," *Current Robot. Rep.*, vol. 3, no. 4, pp. 213–225, Aug. 2022.
[4] A. Prorok, M. Malencia, L. Carlone, G. S. Sukhatme, B. M. Sadler, and V. Kumar, "Beyond robustness: A taxonomy of approaches towards resilient multi-robot systems," 2021, *arXiv:2109.12343*.
[5] J. Gregory, J. Fink, E. Stump, J. Twigg, J. Rogers, D. Baran, N. Fung, and S. Young, *Application of Multi-Robot Systems to Disaster-Relief Scenarios With Limited Communication*. Cham, Switzerland: Springer, 2016, pp. 639–653.
[6] J. Stephan, J. Fink, V. Kumar, and A. Ribeiro, "Concurrent control of mobility and communication in multirobot systems," *IEEE Trans. Robot.*, vol. 33, no. 5, pp. 1248–1254, Oct. 2017.
[7] D. Mox, M. Calvo-Fullana, M. Gerasimenko, J. Fink, V. Kumar, and A. Ribeiro, "Mobile wireless network infrastructure on demand," in *Proc. IEEE Int. Conf. Robot. Autom. (ICRA)*, May 2020, pp. 7726–7732.
[8] J. S. Baras, P. Hovareshti, and H. Chen, "Motif-based communication network formation for task specific collaboration in complex environments," in *Proc. Amer. Control Conf.*, Jun. 2011, pp. 1051–1056.
[9] D. Mox, V. Kumar, and A. Ribeiro, "Learning connectivity-maximizing network configurations," *IEEE Robot. Autom. Lett.*, vol. 7, no. 2, pp. 5552–5559, Apr. 2022.
[10] A. Fotouhi, H. Qiang, M. Ding, M. Hassan, L. G. Giordano, A. Garcia-Rodriguez, and J. Yuan, "Survey on UAV cellular communications: Practical aspects, standardization advancements, regulation, and security challenges," *IEEE Commun. Surveys Tuts.*, vol. 21, no. 4, pp. 3417–3442, 4th Quart., 2019.
[11] Y. Wu, B. Zhang, X. Yi, and Y. Tang, "Communication-motion planning for wireless relay-assisted multi-robot system," *IEEE Wireless Commun. Lett.*, vol. 5, no. 6, pp. 568–571, Dec. 2016.
[12] R. Li, Y. Xiao, P. Yang, W. Tang, M. Wu, and Y. Gao, "UAV-aided two-way relaying for wireless communications of intelligent robot swarms," *IEEE Access*, vol. 8, pp. 56141–56150, 2020.
[13] I. A. Hemadeh, K. Satyanarayana, M. El-Hajjar, and L. Hanzo, "Millimeter-wave communications: Physical channel models, design considerations, antenna constructions, and link-budget," *IEEE Commun. Surveys Tuts.*, vol. 20, no. 2, pp. 870–913, 2nd Quart., 2018.
[14] E. A. Stump and B. M. Sadler, "Persistent surveillance using mutually-visible robotic formations," *Proc. SPIE*, vol. 7694, p. 76940, May 2010.
[15] M. Conti and S. Giordano, "Mobile ad hoc networking: Milestones, challenges, and new research directions," *IEEE Commun. Mag.*, vol. 52, no. 1, pp. 85–96, Jan. 2014.
[16] B. Karp and H.-T. Kung, "GPSR: Greedy perimeter stateless routing for wireless networks," in *Proc. 6th Annu. Int. Conf. Mobile Comput. Netw.*, 2000, pp. 243–254.
[17] M. Heissenbüttel, T. Braun, T. Bernoulli, and M. Wälchli, "BLR: Beacon-less routing algorithm for mobile ad hoc networks," *Comput. Commun.*, vol. 27, no. 11, pp. 1076–1086, Jul. 2004.

[18] Z. Zhao, D. Rosário, T. Braun, and E. Cerqueira, "Context-aware opportunistic routing in mobile ad-hoc networks incorporating node mobility," in *Proc. IEEE Wireless Commun. Netw. Conf. (WCNC)*, Apr. 2014, pp. 2138–2143.

[19] Q. Zhao and B. M. Sadler, "A survey of dynamic spectrum access," *IEEE Signal Process. Mag.*, vol. 24, no. 3, pp. 79–89, May 2007.

[20] S. Geirhofer, L. Tong, and B. Sadler, "Cognitive radios for dynamic spectrum access–dynamic spectrum access in the time domain: Modeling and exploiting white space," *IEEE Commun. Mag.*, vol. 45, no. 5, pp. 66–72, May 2007.

[21] X. Yu, D. Saldaña, D. Shishika, and M. A. Hsieh, "Resilient consensus in robot swarms with periodic motion and intermittent communication," *IEEE Trans. Robot.*, vol. 38, no. 1, pp. 110–125, Feb. 2022.

[22] P. Yu, J. Twigg, B. M. Sadler, and J. Fink, "Exploiting RSS between two moving agents to maintain connectivity," in *Proc. 11th Int. Symp. Distrib. Auto. Robot. Syst.*, 2012.

[23] B. Madhevan and M. Sreekumar, "Tracking algorithm using leader follower approach for multi robots," *Proc. Eng.*, vol. 64, pp. 1426–1435, Jan. 2013.

[24] J. Fink, J. Twigg, P. Yu, and B. M. Sadler, "A parsimonious model for wireless connectivity in robotic networks," in *Proc. IEEE Global Conf. Signal Inf. Process.*, Dec. 2013, pp. 855–858.

[25] J. Fink, A. Ribeiro, and V. Kumar, "Robust control of mobility and communications in autonomous robot teams," *IEEE Access*, vol. 1, pp. 290–309, 2013.

[26] J. N. Twigg, J. R. Fink, P. L. Yu, and B. M. Sadler, "Efficient base station connectivity area discovery," *Int. J. Robot. Res.*, vol. 32, no. 12, pp. 1398–1410, Oct. 2013, doi: 10.1177/0278364913488634.

[27] F. Bullo, J. Cortés, and S. Martínez, *Distributed Control of Robotic Networks: A Mathematical Approach to Motion Coordination Algorithms*. Princeton, NJ, USA: Princeton Univ. Press, 2009.

[28] A. Nedic, A. Olshevsky, and M. G. Rabbat, "Network topology and communication-computation tradeoffs in decentralized optimization," *Proc. IEEE*, vol. 106, no. 5, pp. 953–976, May 2018.

[29] T. Li, M. Fu, L. Xie, and J.-F. Zhang, "Distributed consensus with limited communication data rate," *IEEE Trans. Autom. Control*, vol. 56, no. 2, pp. 279–292, Feb. 2011.

[30] A. Koppel, B. M. Sadler, and A. Ribeiro, "Proximity without consensus in online multiagent optimization," *IEEE Trans. Signal Process.*, vol. 65, no. 12, pp. 3062–3077, Jun. 2017.

[31] H. G. Tanner, A. Jadbabaie, and G. J. Pappas, "Flocking in fixed and switching networks," *IEEE Trans. Autom. Control*, vol. 52, no. 5, pp. 863–868, May 2007.

[32] L. Wang and F. Xiao, "Finite-time consensus problems for networks of dynamic agents," *IEEE Trans. Autom. Control*, vol. 55, no. 4, pp. 950–955, Apr. 2010.

[33] M. M. Zavlanos, M. B. Egerstedt, and G. J. Pappas, "Graph-theoretic connectivity control of mobile robot networks," *Proc. IEEE*, vol. 99, no. 9, pp. 1525–1540, Sep. 2011.

[34] E. Tolstaya, F. Gama, J. Paulos, G. Pappas, V. Kumar, and A. Ribeiro, "Learning decentralized controllers for robot swarms with graph neural networks," in *Proc. Conf. Robot Learn.* (Proceedings of Machine Learning Research), vol. 100, L. P. Kaelbling, D. Kragic, and K. Sugiura, Eds. PMLR, Oct./Nov. 2020, pp. 671–682. [Online]. Available: https://proceedings.mlr.press/v100/tolstaya20a.html

[35] T.-K. Hu, F. Gama, T. Chen, W. Zheng, Z. Wang, A. Ribeiro, and B. M. Sadler, "Scalable perception-action-communication loops with convolutional and graph neural networks," *IEEE Trans. Signal Inf. Process. Over Netw.*, vol. 8, pp. 12–24, 2022.

[36] M. Tzes, N. Bousias, E. Chatzipantazis, and G. J. Pappas, "Graph neural networks for multi-robot active information acquisition," in *Proc. IEEE Int. Conf. Robot. Autom. (ICRA)*, May 2023, pp. 3497–3503.

[37] M. Lauri, D. Hsu, and J. Pajarinen, "Partially observable Markov decision processes in robotics: A survey," *IEEE Trans. Robot.*, vol. 39, no. 1, pp. 21–40, Feb. 2023.

[38] (2023). *Radio Spectrum*. [Online]. Available: https://en.wikipedia.org/wiki/Radio_spectrum

[39] (2023). *International Telecommunications Union*. [Online]. Available: http://www.itu.int

[40] Federal Commun. commission. (2023). *Federal Communications Commission*. [Online]. Available: https://www.fcc.gov/engineering-technology/policy-and-rules-division/general/radio-spectrum-allocation

[41] A. U. Chaudhry and R. H. M. Hafez, "LMR and LTE for public safety in 700 MHz spectrum," *Wireless Commun. Mobile Comput.*, vol. 2019, pp. 1–17, Jun. 2019.

[42] A. Kumbhar, F. Koohifar, I. Güvenç, and B. Mueller, "A survey on legacy and emerging technologies for public safety communications," *IEEE Commun. Surveys Tuts.*, vol. 19, no. 1, pp. 97–124, 1st Quart., 2017.

[43] W. Yu, H. Xu, J. Nguyen, E. Blasch, A. Hematian, and W. Gao, "Survey of public safety communications: User-side and network-side solutions and future directions," *IEEE Access*, vol. 6, pp. 70397–70425, 2018.

[44] A. Jarwan, A. Sabbah, M. Ibnkahla, and O. Issa, "LTE-based public safety networks: A survey," *IEEE Commun. Surveys Tuts.*, vol. 21, no. 2, pp. 1165–1187, 2nd Quart., 2019.

[45] S. W. Choi, Y.-S. Song, W.-Y. Shin, and J. Kim, "A feasibility study on mission-critical push-to-talk: Standards and implementation perspectives," *IEEE Commun. Mag.*, vol. 57, no. 2, pp. 81–87, Feb. 2019.

[46] Y. Jahir, M. Atiquzzaman, H. Refai, A. Paranjothi, and P. G. LoPresti, "Routing protocols and architecture for disaster area network: A survey," *Ad Hoc Netw.*, vol. 82, pp. 1–14, Jan. 2019.

[47] J. D. Parsons, *The Mobile Radio Propagation Channel*. Hoboken, NJ, USA: Wiley, 2000.

[48] R. G. Kouyoumjian, "Asymptotic high-frequency methods," *Proc. IEEE*, vol. 53, no. 8, pp. 864–876, May 1965.

[49] G. Ding, Y. Jiao, J. Wang, Y. Zou, Q. Wu, Y. D. Yao, and L. Hanzo, "Spectrum inference in cognitive radio networks: Algorithms and applications," *IEEE Commun. Surveys Tuts.*, vol. 20, no. 1, pp. 150–182, 1st Quart., 2018.

[50] H. Ohara, H. Sawada, M. Oodo, H. Kobayashi, F. Kojima, H. Harada, and J.-I. Takada, "Power delay profile measurement for VHF-band broadband mobile communication system," in *Proc. IEEE 27th Annu. Int. Symp. Pers., Indoor, Mobile Radio Commun. (PIMRC)*, Sep. 2016, pp. 1–6.

[51] N. Faruk, S. I. Popoola, N. T. Surajudeen-Bakinde, A. A. Oloyede, A. Abdulkarim, L. A. Olawoyin, M. Ali, C. T. Calafate, and A. A. Atayero, "Path loss predictions in the VHF and UHF bands within urban environments: Experimental investigation of empirical, heuristics and geospatial models," *IEEE Access*, vol. 7, pp. 77293–77307, 2019.

[52] E. V. Muñoz, L. da Silva Mello, and M. P. C. Almeida, "Results of medium wave HD radio mobile reception measurements in a dense urban region," in *Proc. 12th Eur. Conf. Antennas Propag. (EuCAP)*, 2018, pp. 1–5.

[53] S. I. Popoola, A. Jefia, A. A. Atayero, O. Kingsley, N. Faruk, O. F. Oseni, and R. O. Abolade, "Determination of neural network parameters for path loss prediction in very high frequency wireless channel," *IEEE Access*, vol. 7, pp. 150462–150483, 2019.

[54] H. Kyu Chung and H. L. Bertoni, "Range-dependent path-loss model in residential areas for the VHF and UHF bands," *IEEE Trans. Antennas Propag.*, vol. 50, no. 1, pp. 1–11, Nov. 2002.

[55] J. Kim, A. Oguntade, M. Oza, and S. Kim, "Range estimation of tactical radio waveforms using link budget analysis," in *Proc. IEEE Mil. Commun. Conf.*, Oct. 2009, pp. 1–7.

[56] J. R. Hampton, N. M. Merheb, W. L. Lain, D. E. Paunil, R. M. Shuford, and W. T. Kasch, "Urban propagation measurements for ground based communication in the military UHF band," *IEEE Trans. Antennas Propag.*, vol. 54, no. 2, pp. 644–654, Feb. 2006.

[57] J. Andrusenko, R. L. Miller, J. A. Abrahamson, N. M. Merheb Emanuelli, R. S. Pattay, and R. M. Shuford, "VHF general urban path loss model for short range ground-to-ground communications," *IEEE Trans. Antennas Propag.*, vol. 56, no. 10, pp. 3302–3310, Oct. 2008.

[58] M. Suchanski, P. Kaniewski, R. Matyszkiel, and P. Gajewski, "Prediction of VHF and UHF wave attenuation in urban environment," in *Proc. 19th Int. Conf. Microw., Radar Wireless Commun.*, May 2012, pp. 60–65.

[59] D. P. Wright and E. A. Ball, "IoT focused VHF and UHF propagation study and comparisons," *IET Microw., Antennas Propag.*, vol. 15, no. 8, pp. 871–884, Jul. 2021.

[60] E. Bedeer, J. Pugh, C. Brown, and H. Yanikomeroglu, "Measurement-based path loss and delay spread propagation models in VHF/UHF bands for IoT communications," in *Proc. IEEE 86th Veh. Technol. Conf.*, Sep. 2017, pp. 1–5.

[61] J. Pugh, R. Bultitude, and P. Vigneron, "Path loss measurements with low antennas for segmented wideband communications at VHF," in *Proc. MILCOM*, Oct. 2006, pp. 1–4.

[62] J. A. Pugh, R. J. C. Bultitude, and P. J. Vigneron, "Propagation measurements and modelling for multiband communications on tactical VHF channels," in *Proc. IEEE Mil. Commun. Conf.*, Oct. 2007, pp. 1–7.

[63] J. Fischer, M. Grossmann, W. Felber, M. Landmann, and A. Heuberger, "A novel delay spread distribution model for VHF and UHF mobile-to-mobile channels," in *Proc. 7th Eur. Conf. Antennas Propag. (EuCAP)*, 2013, pp. 469–472.
[64] P. J. Vigneron and J. A. Pugh, "Propagation models for mobile terrestrial VHF communications," in *Proc. IEEE Mil. Commun. Conf.*, Nov. 2008, pp. 1–7.
[65] K. Sabet, A. I. Stefan, K. Sarabandi, F. Dagefu, and B. M. Sadler, "Highly parallelized hybrid FDTD solver for simulating electromagnetic wave propagation in dense urban environments," in *Proc. IEEE Int. Symp. Antennas Propag. USNC-URSI Radio Sci. Meeting (APS/URSI)*, Dec. 2021, pp. 1097–1098.
[66] (2014). *Handbook on Ground Wave Propagation*. [Online]. Available: http://handle.itu.int/11.1002/pub/809efe7d-en
[67] J. Wang, H. Zhou, Y. Li, Q. Sun, Y. Wu, S. Jin, T. Q. S. Quek, and C. Xu, "Wireless channel models for maritime communications," *IEEE Access*, vol. 6, pp. 68070–68088, 2018.
[68] D. Green, J. K. E. Tunaley, C. Fowler, and D. Power, "VHF propagation study," Defence R&D Canada—Atlantic, Ottawa, ON, Canada, Tech. Rep., DRDC Atlantic CR 2011-152, 2011.
[69] D. Liao and K. Sarabandi, "Near-earth wave propagation characteristics of electric dipole in presence of vegetation or snow layer," *IEEE Trans. Antennas Propag.*, vol. 53, no. 11, pp. 3747–3756, Nov. 2005.
[70] D. Liao and K. Sarabandi, "Terminal-to-terminal hybrid full-wave simulation of low-profile, electrically-small, near-ground antennas," *IEEE Trans. Antennas Propag.*, vol. 56, no. 3, pp. 806–814, Mar. 2008.
[71] F. T. Dagefu and K. Sarabandi, "Analysis and modeling of near-ground wave propagation in the presence of building walls," *IEEE Trans. Antennas Propag.*, vol. 59, no. 6, pp. 2368–2378, Jun. 2011.
[72] M. Sheikhsofla and K. Sarabandi, "Indoor wave propagation simulations at HF using Rayleigh-gans approximation," in *Proc. USNC-URSI Radio Sci. Meeting*, Jul. 2013, p. 202.
[73] M. Sheikhsofla and K. Sarabandi, "Indoor wave propagation modeling at low-VHF band," in *Proc. IEEE-APS Topical Conf. Antennas Propag. Wireless Commun. (APWC)*, Aug. 2014, pp. 778–781.
[74] D. Dres, D. Vouyioukas, D. Triantafilidis, and P. Constantinou, "Building penetration measurements for 2.4 GHz broadcasting CDMA system," in *Proc. Gateway 21st Century Commun. Village, VTC -Fall, IEEE VTS 50th Veh. Technol. Conf.*, 1999, pp. 1982–1987.
[75] W. F. Young, C. L. Holloway, G. Koepke, D. Camell, Y. Becquet, and K. A. Remley, "Radio-wave propagation into large building structures—Part 1: CW signal attenuation and variability," *IEEE Trans. Antennas Propag.*, vol. 58, no. 4, pp. 1279–1289, Apr. 2010.
[76] C. L. Holloway, G. Koepke, D. Camell, W. F. Young, and K. A. Remley, "Propagation measurements before, during, and after the collapse of three large public buildings," *IEEE Antennas Propag. Mag.*, vol. 56, no. 3, pp. 16–36, Jun. 2014.
[77] W. Turney, M. Karam, L. Malek, and G. Buchwald, "VHF/UHF building penetration characteristics when using low antenna heights," in *Proc. 2nd IEEE Int. Symp. New Frontiers Dyn. Spectr. Access Netw.*, Apr. 2007, pp. 664–675.
[78] M. Karam, W. Turney, K. L. Baum, P. J. Sartori, L. Malek, and I. Ould-Dellahy, "Outdoor-indoor propagation measurements and link performance in the VHF/UHF bands," in *Proc. IEEE 68th Veh. Technol. Conf.*, Sep. 2008, pp. 1–5.
[79] R. Zabela and C. W. Bostian, "Measurements of building penetration by low orbit satellite signals at VHF," in *IEEE Antennas Propag. Soc. Int. Symp. Dig.*, Feb. 1992, pp. 604–607.
[80] R. A. Dalke, C. L. Holloway, P. McKenna, M. Johansson, and A. S. Ali, "Effects of reinforced concrete structures on RF communications," *IEEE Trans. Electromagn. Compat.*, vol. 42, no. 4, pp. 486–496, Mar. 2000.
[81] M. Orefice and G. C. Vietti, "Transparency of buildings to the radiowave propagation at VHF-UHF frequencies," in *Proc. 6th Eur. Conf. Antennas Propag. (EUCAP)*, Mar. 2012, pp. 2418–2421.
[82] M. Orefice, "Analysis of the propagation attenuation from large buildings in broadcasting services," in *Proc. 9th Eur. Conf. Antennas Propag. (EuCAP)*, Apr. 2015, pp. 1–5.
[83] F. T. Dagefu, G. Verma, C. R. Rao, P. L. Yu, J. R. Fink, B. M. Sadler, and K. Sarabandi, "Short-range low-VHF channel characterization in cluttered environments," *IEEE Trans. Antennas Propag.*, vol. 63, no. 6, pp. 2719–2727, Jun. 2015.
[84] F. T. Dagefu, J. Choi, M. Sheikhsofla, B. M. Sadler, and K. Sarabandi, "Performance assessment of lower VHF band for short-range communication and geolocation applications," *Radio Sci.*, vol. 50, no. 5, pp. 443–452, May 2015.
[85] F. T. Dagefu, G. Verma, C. R. Rao, P. L. Yu, J. R. Fink, B. M. Sadler, and K. Sarabandi, "Low VHF channel measurements and simulations in indoor and outdoor scenarios," Army Res. Lab., Adelphi, MD, USA, Tech. Rep., ARL-TR-7282, May 2015.
[86] J. Choi, F. T. Dagefu, B. M. Sadler, and K. Sarabandi, "Low-power low-VHF ad-hoc networking in complex environments," *IEEE Access*, vol. 5, pp. 24120–24127, 2017.
[87] J. Choi, C. Rao, and F. T. Dagefu, "Real-time digital video streaming at low-VHF for compact autonomous agents in complex scenes," in *Proc. IEEE 89th Veh. Technol. Conf.*, Apr. 2019, pp. 1–5.
[88] F. T. Dagefu, J. Choi, B. M. Sadler, and K. Sarabandi, "A survey of small, low-frequency antennas: Recent designs, practical challenges, and research directions," *IEEE Antennas Propag. Mag.*, vol. 65, no. 1, pp. 14–26, Feb. 2023.
[89] J. Choi, F. T. Dagefu, B. M. Sadler, and K. Sarabandi, "A miniature actively matched antenna for power-efficient and bandwidth-enhanced operation at low VHF," *IEEE Trans. Antennas Propag.*, vol. 69, no. 1, pp. 556–561, Jan. 2021.
[90] J. G. Rogers, C. Nieto-Granda, and H. I. Christensen, *Coordination Strategies for Multi-robot Exploration and Mapping*. Heidelberg, Germany: Springer, 2013, pp. 231–243.
[91] S. Mokssit, D. B. Licea, B. Guermah, and M. Ghogho, "Deep learning techniques for visual SLAM: A survey," *IEEE Access*, vol. 11, pp. 20026–20050, 2023.
[92] A. Cramariuc, L. Bernreiter, F. Tschopp, M. Fehr, V. Reijgwart, J. Nieto, R. Siegwart, and C. Cadena, "Maplab 2.0—A modular and multi-modal mapping framework," *IEEE Robot. Autom. Lett.*, vol. 8, no. 2, pp. 520–527, Feb. 2023.
[93] J. A. Placed, J. Strader, H. Carrillo, N. Atanasov, V. Indelman, L. Carlone, and J. A. Castellanos, "A survey on active simultaneous localization and mapping: State of the art and new frontiers," *IEEE Trans. Robot.*, vol. 39, no. 3, pp. 1686–1705, Jun. 2023.
[94] N. Patwari, J. N. Ash, S. Kyperountas, A. O. Hero, R. L. Moses, and N. S. Correal, "Locating the nodes: Cooperative localization in wireless sensor networks," *IEEE Signal Process. Mag.*, vol. 22, no. 4, pp. 54–69, Jul. 2005.
[95] A. S. M. Prorok, "Models and algorithms for ultra-wideband localization in single- and multi-robot systems," Ph.D. thesis, EPFL, 2013. [Online]. Available: https://infoscience.epfl.ch/record/186761?ln=en
[96] J. González, J. L. Blanco, C. Galindo, A. Ortiz-de-Galisteo, J. A. Fernández-Madrigal, F. A. Moreno, and J. L. Martínez, "Mobile robot localization based on ultra-wide-band ranging: A particle filter approach," *Robot. Auto. Syst.*, vol. 57, no. 5, pp. 496–507, May 2009.
[97] F. Zafari, A. Gkelias, and K. K. Leung, "A survey of indoor localization systems and technologies," *IEEE Commun. Surveys Tuts.*, vol. 21, no. 3, pp. 2568–2599, 3rd Quart., 2019.
[98] S. Srinivas, A. Herschfelt, A. Chiriyath, and D. W. Bliss, "Joint positioning-communications: Constant-information ranging for dynamic spectrum access," in *Proc. IEEE 92nd Veh. Technol. Conf. (VTC-Fall)*, Nov. 2020, pp. 1–5.
[99] S. Srinivas, A. Herschfelt, H. Yu, S. Wu, Y. Li, H. Lee, C. Chakrabarti, and D. W. Bliss, "Communications and high-precision positioning (CHP2): Enabling secure CNS and APNT for safety-critical air transport systems," in *Proc. AIAA/IEEE 39th Digit. Avionics Syst. Conf. (DASC)*, Oct. 2020, pp. 1–6.
[100] F. T. Dagefu, J. Oh, and K. Sarabandi, "A sub-wavelength RF source tracking system for GPS-denied environments," *IEEE Trans. Antennas Propag.*, vol. 61, no. 4, pp. 2252–2262, Apr. 2013.
[101] F. T. Dagefu, G. Verma, B. M. Sadler, R. Kozick, and K. Sarabandi, "Full-wave analysis of time of arrival based localization with polarization diversity," in *Proc. USNC-URSI Radio Sci. Meeting*, Jul. 2017, pp. 5–6.
[102] F. T. Dagefu and K. Sarabandi, "High resolution subsurface imaging of deep targets based on distributed sensor networks," in *Proc. IEEE Int. Geosci. Remote Sens. Symp.*, May 2009, pp. 1–11.
[103] F. T. Dagefu and K. Sarabandi, "Soil dielectric and senisitivity analysis for subsurface imaging applications based on distributed sensor networks," in *Proc. IEEE Int. Geosci. Remote Sens. Symp.*, Jul. 2010, pp. 1839–1842.

[104] F. T. Dagefu and K. Sarabandi, "A 3D subsurface imaging technique based on distributed near-ground sensors: Investigation using scale model measurements," in *Proc. IEEE Int. Geosci. Remote Sens. Symp.*, Jul. 2011, pp. 882–885.

[105] F. T. Dagefu and K. Sarabandi, "High-resolution subsurface imaging of deeply submerged targets based on distributed near-ground sensors," *IEEE Trans. Geosci. Remote Sens.*, vol. 52, no. 2, pp. 1089–1098, Feb. 2014.

[106] J. N. Twigg, J. R. Fink, P. L. Yu, and B. M. Sadler, "RSS gradient-assisted frontier exploration and radio source localization," in *Proc. IEEE Int. Conf. Robot. Automat.*, 2012, pp. 889–895.

[107] A. Wadhwa, U. Madhow, J. Hespanha, and B. M. Sadler, "Following an RF trail to its source," in *Proc. 49th Annu. Allerton Conf. Commun., Control, Comput. (Allerton)*, Sep. 2011, pp. 580–587.

[108] G. Verma, F. T. Dagefu, B. M. Sadler, and J. Twigg, "Direction of arrival estimation with the received signal strength gradient," *IEEE Trans. Veh. Technol.*, vol. 67, no. 11, pp. 10856–10870, Nov. 2018.

[109] G. Verma, F. Dagefu, B. M. Sadler, J. Twigg, and J. Fink, "DOA estimation for autonomous systems in complex propagation environments," in *Proc. IEEE 19th Int. Workshop Signal Process. Adv. Wireless Commun. (SPAWC)*, Jun. 2018, pp. 1–5.

[110] S. Jayaprakasam, S. K. A. Rahim, and C. Y. Leow, "Distributed and collaborative beamforming in wireless sensor networks: Classifications, trends, and research directions," *IEEE Commun. Surveys Tuts.*, vol. 19, no. 4, pp. 2092–2116, 4th Quart., 2017.

[111] R. Mudumbai, D. R. Brown, U. Madhow, and H. V. Poor, "Distributed transmit beamforming: Challenges and recent progress," *IEEE Commun. Mag.*, vol. 47, no. 2, pp. 102–110, Feb. 2009.

[112] I. Ahmad, C. K. Sung, D. Kramarev, G. Lechner, H. Suzuki, and I. Grivell, "Outage probability and ergodic capacity of distributed transmit beamforming with imperfect CSI," *IEEE Trans. Veh. Technol.*, vol. 71, no. 3, pp. 3008–3019, Mar. 2022.

[113] Y. Savas, E. Noorani, A. Koppel, J. Baras, U. Topcu, and B. M. Sadler, "Collaborative one-shot beamforming under localization errors: A discrete optimization approach," *Signal Process.*, vol. 200, Nov. 2022, Art. no. 108647.

[114] E. Noorani, Y. Savas, A. Koppel, J. Baras, U. Topcu, and B. M. Sadler, "Collaborative beamforming for agents with localization errors," in *Proc. 55th Asilomar Conf. Signals, Syst., Comput.*, Oct. 2021, pp. 204–208.

[115] R. Mudumbai, J. Hespanha, U. Madhow, and G. Barriac, "Distributed transmit beamforming using feedback control," *IEEE Trans. Inf. Theory*, vol. 56, no. 1, pp. 411–426, Jan. 2010.

[116] M. J. Grabner, F. T. Dagefu, J. N. Twigg, B. Azimi-Sadjadi, and B. M. Sadler, "Calibration of multi-robot coherent beamforming," in *Proc. Int. Conf. Mil. Commun. Inf. Syst. (ICMCIS)*, 2023, pp 1–6, doi: 10.1109/ICMCIS59922.2023.10253596.

[117] J. Kong, F. T. Dagefu, and B. M. Sadler, "Distributed beamforming in the presence of adversaries," *IEEE Trans. Veh. Technol.*, vol. 69, no. 9, pp. 9682–9696, Sep. 2020.

[118] Y. Savas, A. Hashemi, A. P. Vinod, B. M. Sadler, and U. Topcu, "Physical-layer security via distributed beamforming in the presence of adversaries with unknown locations," in *Proc. IEEE Int. Conf. Acoust., Speech Signal Process. (ICASSP)*, Jun. 2021, pp. 4685–4689.

[119] J. Kong, F. T. Dagefu, and B. M. Sadler, "Multi-group distributed nullforming and sectorized jamming," *IEEE Trans. Veh. Technol.*, vol. 70, no. 9, pp. 9572–9576, Sep. 2021.

[120] J. Kong, F. T. Dagefu, and B. M. Sadler, "Coverage analysis of distributed beamforming with random phase offsets using Ginibre point process," *IEEE Access*, vol. 8, pp. 134351–134362, 2020.

[121] C. A. Balanis, *Antenna Theory Analysis and Design*, 3rd ed. Hoboken, NJ, USA: Wiley, 2005.

[122] K. Iigusa, K. Sato, and M. Fujise, "A slim electronically steerable parasitic array radiator antenna," in *Proc. 6th Int. Conf. ITS Telecommun.*, Jun. 2006, pp. 386–389.

[123] S. Panagiotou, T. Dimousios, S. Mitilineos, and C. Capsalis, "Broadband switched parasitic arrays for portable DVB-T receiver applications in the VHF/UHF bands," *IEEE Antennas Propag. Mag.*, vol. 50, no. 5, pp. 110–117, Oct. 2008.

[124] S. C. Panagiotou, S. A. Mitilineos, T. D. Dimousios, and C. N. Capsalis, "A broadband, vertically polarized, circular switched parasitic array for indoor portable DVB-T applications at the IV UHF band," *IEEE Trans. Broadcast.*, vol. 53, no. 2, pp. 547–552, Jun. 2007.

[125] J. Twigg, F. Dagefu, N. Chopra, and B. M. Sadler, "Robotic parasitic array optimization in outdoor environments," in *Proc. IEEE Int. Symp. Saf., Secur., Rescue Robot. (SSRR)*, Sep. 2019, pp. 1–8.

[126] F. T. Dagefu, J. N. Twigg, C. R. Rao, and B. M. Sadler, "Directional communication enabled by mobile parasitic elements," in *Proc. Int. Conf. Mil. Commun. Inf. Syst. (ICMCIS)*, May 2019, pp. 1–7.

[127] J. D. Kraus, R. J. Marhefka, and A. S. Khan, *Antennas for All Applications*. New York, NY, USA: McGraw-Hill, 2002.

[128] J. N. Twigg, F. T. Dagefu, N. Chopra, and B. M. Sadler, "Robotic parasitic array control for increased RSS in non-line-of-sight," *IEEE Robot. Autom. Lett.*, vol. 7, no. 4, pp. 9167–9174, Oct. 2022.

[129] J. N. Twigg, N. Chopra, and B. M. Sadler, "Communication maintenance of robotic parasitic antenna arrays," *IEEE Robot. Autom. Lett.*, vol. 5, no. 4, pp. 6475–6482, Oct. 2020.

[130] M. T. Ivrlac and J. A. Nossek, "The multiport communication theory," *IEEE Circuits Syst. Mag.*, vol. 14, no. 3, pp. 27–44, 3rd Quart., 2014.

[131] J. C. Coetzee and Y. Yu, "Design of decoupling networks for circulant symmetric antenna arrays," *IEEE Antennas Wireless Propag. Lett.*, vol. 8, pp. 291–294, 2009.

[132] J. Weber, C. Volmer, K. Blau, R. Stephan, and M. A. Hein, "Miniaturized antenna arrays using decoupling networks with realistic elements," *IEEE Trans. Microw. Theory Techn.*, vol. 54, no. 6, pp. 2733–2740, Jun. 2006.

[133] D. Nie, B. M. Hochwald, and E. Stauffer, "Systematic design of large-scale multiport decoupling networks," *IEEE Trans. Circuits Syst. I, Reg. Papers*, vol. 61, no. 7, pp. 2172–2181, Jul. 2014.

[134] C. Volmer, J. Weber, R. Stephan, K. Blau, and M. A. Hein, "An eigen-analysis of compact antenna arrays and its application to port decoupling," *IEEE Trans. Antennas Propag.*, vol. 56, no. 2, pp. 360–370, Jan. 2008.

[135] Y. Zang, H. Luyen, H. R. Bahrami, and N. Behdad, "An analytic synthesis method for two-element biomimetic antenna arrays," *IEEE Trans. Antennas Propag.*, vol. 68, no. 4, pp. 2797–2809, Apr. 2020.

[136] F. Pereira, J. Nossek, and F. Cavalcanti, "Decoupling and matching strategies for compact antenna arrays," *J. Commun. Inf. Syst.*, vol. 35, no. 1, pp. 290–299, 2020.

[137] M. J. Gans, "Channel capacity between antenna arrays—Part I: Sky noise dominates," *IEEE Trans. Commun.*, vol. 54, no. 9, pp. 1586–1592, Sep. 2006.

[138] K. F. Warnick and M. A. Jensen, "Optimal noise matching for mutually coupled arrays," *IEEE Trans. Antennas Propag.*, vol. 55, no. 6, pp. 1726–1731, Jun. 2007.

[139] N. Barani, J. F. Harvey, and K. Sarabandi, "Fragmented antenna realization using coupled small radiating elements," *IEEE Trans. Antennas Propag.*, vol. 66, no. 4, pp. 1725–1735, Apr. 2018.

[140] B. K. Lau and J. B. Andersen, "Simple and efficient decoupling of compact arrays with parasitic scatterers," *IEEE Trans. Antennas Propag.*, vol. 60, no. 2, pp. 464–472, Feb. 2012.

[141] S. Salama and K. Solbach, "Parasitic elements based decoupling technique for monopole four square array antenna," in *Proc. 44th Eur. Microw. Conf.*, Oct. 2014, pp. 1504–1507.

[142] J. Choi and F. T. Dagefu, "A low-profile, top-loaded, multielement, monopole antenna for compact UGV systems," *IEEE Trans. Antennas Propag.*, vol. 70, no. 3, pp. 2277–2282, Mar. 2022.

[143] R. J. Kozick, F. T. Dagefu, and B. M. Sadler, "Performance metrics for biomimetic antenna array (BMAA) systems," in *Proc. IEEE Int. Symp. Antennas Propag. USNC-URSI Radio Sci. Meeting (USNC-URSI)*, 2023, pp. 1629–1630, doi: 10.1109/USNC-URSI52151.2023.10237657.

[144] R. J. Kozick, F. T. Dagefu, and B. M. Sadler, "Two-element biomimetic antenna array design and performance," in *Proc. IEEE Int. Conf. Acoust., Speech Signal Process. (ICASSP)*, May 2020, pp. 4747–4751.

[145] M. Ranjbar Nikkhah, K. Ghaemi, and N. Behdad, "A three-element biomimetic antenna array with an electrically small triangular lattice," *IEEE Trans. Antennas Propag.*, vol. 65, no. 8, pp. 4007–4016, Aug. 2017.

[146] R. C. Hansen, "Fundamental limitations in antennas," *Proc. IEEE*, vol. 69, no. 2, pp. 170–182, Feb. 1981.

[147] R. P. Haviland, "Supergain antennas: Possibilities and problems," *IEEE Antennas Propag. Mag.*, vol. 37, no. 4, pp. 13–26, Apr. 1995.

[148] T. L. Marzetta, "Super-directive antenna arrays: Fundamentals and new perspectives," in *Proc. 53rd Asilomar Conf. Signals, Syst., Comput.*, Nov. 2019, pp. 1–4.

[149] A. Kisliansky, R. Shavit, and J. Tabrikian, "Direction of arrival estimation in the presence of noise coupling in antenna arrays," *IEEE Trans. Antennas Propag.*, vol. 55, no. 7, pp. 1940–1947, Jul. 2007.

[150] H. J. Chaloupka, X. Wang, and J. C. Coetzee, "A superdirective 3-element array for adaptive beamforming," *Microw. Opt. Technol. Lett.*, vol. 36, no. 6, pp. 425–430, 2003.
[151] L. Han, H. Yin, and T. L. Marzetta, "Coupling matrix-based beamforming for superdirective antenna arrays," in *Proc. IEEE Int. Conf. Commun. (ICC)*, May 2022, pp. 5159–5164.
[152] L. Han, H. Yin, M. Gao, and J. Xie, "A superdirective beamforming approach with impedance coupling and field coupling for compact antenna arrays," 2023, *arXiv:2302.08203*.
[153] M. L. Morris, M. A. Jensen, and J. W. Wallace, "Superdirectivity in MIMO systems," *IEEE Trans. Antennas Propag.*, vol. 53, no. 9, pp. 2850–2857, Sep. 2005.
[154] N. Bikhazi and M. Jensen, "The relationship between antenna loss and superdirectivity in MIMO systems," *IEEE Trans. Wireless Commun.*, vol. 6, no. 5, pp. 1796–1802, May 2007.
[155] V. Dehghanian and J. Nielsen, "On the capacity of densely packed arrays with mutual coupling and correlated noise," *Int. J. Antennas Propag.*, vol. 2015, pp. 1–12, 2015.
[156] M. Ranjbar Nikkhah, M. A. Panahi, H. Luyen, H. Bahrami, and N. Behdad, "Capacity-enhancement in MIMO systems using biomimetic electrically small antenna arrays," *IET Microw., Antennas Propag.*, vol. 12, no. 13, pp. 2001–2006, 2018.
[157] D. Arceo and C. A. Balanis, "A multiport impedance-matching feed network for directional antennas," *IEEE Antennas Wireless Propag. Lett.*, vol. 11, pp. 1548–1551, 2012.
[158] A. Debard, A. Clemente, A. Tornese, and C. Delaveaud, "On the maximum end-fire directivity of compact antenna arrays based on electrical dipoles and Huygens sources," *IEEE Trans. Antennas Propag.*, vol. 71, no. 1, pp. 299–308, Jan. 2023.
[159] T.-I. Lee and Y. E. Wang, "Mode-based information channels in closely coupled dipole pairs," *IEEE Trans. Antennas Propag.*, vol. 56, no. 12, pp. 3804–3811, Dec. 2008.
[160] M. Pigeon, C. Delaveaud, L. Rudant, and K. Belmkaddem, "Miniature directive antennas," *Int. J. Microw. Wireless Technol.*, vol. 6, no. 1, pp. 45–50, Feb. 2014.
[161] E. E. Altshuler, T. H. O'Donnell, A. D. Yaghjian, and S. R. Best, "A monopole superdirective array," *IEEE Trans. Antennas Propag.*, vol. 53, no. 8, pp. 2653–2661, Aug. 2005.
[162] M. Ranjbar Nikkhah, F. T. Dagefu, and N. Behdad, "Electrically small platform-based antennas for an unmanned ground vehicle," *IEEE Trans. Antennas Propag.*, vol. 68, no. 7, pp. 5189–5198, Jul. 2020.
[163] A. M. Elfrgani and R. G. Rojas, "Biomimetic antenna array using non-foster network to enhance directional sensitivity over broad frequency band," *IEEE Trans. Antennas Propag.*, vol. 64, no. 10, pp. 4297–4305, Oct. 2016.
[164] M. Ranjbar Nikkhah, K. Ghaemi, and N. Behdad, "An electronically tunable biomimetic antenna array," *IEEE Trans. Antennas Propag.*, vol. 66, no. 3, pp. 1248–1257, Mar. 2018.
[165] R. W. Ziolkowski, "The directivity of a compact antenna: An unforgettable figure of merit," *EPJ Appl. Metamater.*, vol. 4, p. 7, Jan. 2017.
[166] T. Kokkinos and A. P. Feresidis, "Electrically small superdirective endfire arrays of metamaterial-inspired low-profile monopoles," *IEEE Antennas Wireless Propag. Lett.*, vol. 11, pp. 568–571, 2012.
[167] R. Pickholtz, L. Milstein, and D. Schilling, "Spread spectrum for mobile communications," *IEEE Trans. Veh. Technol.*, vol. 40, no. 2, pp. 313–322, May 1991.
[168] M. Pursley, "Performance evaluation for phase-coded spread-spectrum multiple-access communication—Part I: System analysis," *IEEE Trans. Commun.*, vol. COM-25, no. 8, pp. 795–799, Aug. 1977.
[169] G. E. Bottomley, "Signature sequence selection in a CDMA system with orthogonal coding," *IEEE Trans. Veh. Technol.*, vol. 42, no. 1, pp. 62–68, Jul. 1993.
[170] S. W. Golomb, *Shift Register Sequences: Secure and Limited-Access Code Generators, Efficiency Code Generators, Prescribed Property Generators, Mathematical Models*, 3rd ed. Singapore: World Scientific Publishing Co., 2017.
[171] P. Z. Fan, N. Suehiro, N. Kuroyanagi, and X. M. Deng, "Class of binary sequences with zero correlation zone," *Electron. Lett.*, vol. 35, no. 10, p. 777, 1999.
[172] P. Fan, "Spreading sequence design and theoretical limits for quasisynchronous CDMA systems," *EURASIP J. Wireless Commun. Netw.*, vol. 2004, no. 1, pp. 19–31, Dec. 2004.
[173] R. De Gaudenzi, C. Elia, and R. Viola, "Bandlimited quasi-synchronous CDMA: A novel satellite access technique for mobile and personal communication systems," *IEEE J. Sel. Areas Commun.*, vol. 10, no. 2, pp. 328–343, Aug. 1992.
[174] V. DaSilva and E. S. Sousa, "Performance of orthogonal CDMA codes for quasi-synchronous communication systems," in *Proc. 2nd IEEE Int. Conf. Universal Pers. Commun.*, Oct. 1993, pp. 995–999.
[175] V. M. DaSilva and E. S. Sousa, "Multicarrier orthogonal CDMA signals for quasi-synchronous communication systems," *IEEE J. Sel. Areas Commun.*, vol. 12, no. 5, pp. 842–852, Jun. 1994.
[176] T.-K. Woo, "Orthogonal code design for quasi-synchronous CDMA," *Electron. Lett.*, vol. 36, no. 19, p. 1632, 2000.
[177] X. Duan Lin and K. Hi Chang, "Optimal PN sequence design for quasisynchronous CDMA communication systems," *IEEE Trans. Commun.*, vol. 45, no. 2, pp. 221–226, Jul. 1997.
[178] K. Choi and H. Liu, "Quasi-synchronous CDMA using properly scrambled Walsh codes as user-spreading sequences," *IEEE Trans. Veh. Technol.*, vol. 59, no. 7, pp. 3609–3617, Sep. 2010.
[179] B. M. Popovic, "Spreading sequences for multicarrier CDMA systems," *IEEE Trans. Commun.*, vol. 47, no. 6, pp. 918–926, Jun. 1999.
[180] R. Prasad and S. Hara, "An overview of multi-carrier CDMA," in *Proc. Int. Symp. Spread Spectr. Techn. Appl.*, Feb. 1996, pp. 107–114.
[181] S. Tsumura and S. Hara, "Design and performance of quasi-synchronous multi-carrier CDMA system," in *Proc. IEEE 54th Veh. Technol. Conf., VTC Fall*, Jan. 2001, pp. 843–847.
[182] K.-W. Yip and T.-S. Ng, "Effects of carrier frequency accuracy on quasi-synchronous, multicarrier DS-CDMA communications using optimized sequences," *IEEE J. Sel. Areas Commun.*, vol. 17, no. 11, pp. 1915–1923, Dec. 1999.
[183] J. Jang and K. Bok Lee, "Effects of frequency offset on MC/CDMA system performance," *IEEE Commun. Lett.*, vol. 3, no. 7, pp. 196–198, Jul. 1999.
[184] G. Verma, F. T. Dagefu, P. Spasojevic, and B. M. Sadler, "Effect of coarse frequency synchrony on spread spectrum codes having a zero correlation zone," in *Wireless Innovation European Conference on Wireless Communications Technologies and Software Defined Radio*. Finland: Univ. of Oulu, 2017. [Online]. Available: https://www.wirelessinnova..on.org/winncomm-europe-2017-proceedings
[185] G. Verma, F. T. Dagefu, B. M. Sadler, and P. Spasojevic, "Implications of time/frequency synchronization tradeoff of quasi-synchronous multi-carrier DS-CDMA for robust communications at lower VHF," in *Proc. IEEE Mil. Commun. Conf.*, Nov. 2016, pp. 694–699.
[186] F. T. Dagefu, G. Verma, P. Spasojevic, and B. M. Sadler, "An experimental study of quasi-synchronous multiuser communications in cluttered scenarios at low VHF," in *Proc. Int. Conf. Mil. Commun. Inf. Syst. (ICMCIS)*, May 2017, pp. 1–7.
[187] F. T. Dagefu, P. Spasojevic, G. Verma, and B. M. Sadler, "The effect of inter-user delay and channel phase response on MC-CDMA using WBE codes with application to lower VHF," in *Proc. 51st Asilomar Conf. Signals, Syst., Comput.*, Oct. 2017, pp. 1737–1741.
[188] P. Viswanath and V. Anantharam, "Optimal sequences and sum capacity of synchronous CDMA systems," *IEEE Trans. Inf. Theory*, vol. 45, no. 6, pp. 1984–1991, Jul. 1999.
[189] M. Rupf and J. L. Massey, "Optimum sequence multisets for synchronous code-division multiple-access channels," *IEEE Trans. Inf. Theory*, vol. 40, no. 4, pp. 1261–1266, Jul. 1994.
[190] L. Dai, B. Wang, Z. Ding, Z. Wang, S. Chen, and L. Hanzo, "A survey of non-orthogonal multiple access for 5G," *IEEE Commun. Surveys Tuts.*, vol. 20, no. 3, pp. 2294–2323, 3rd Quart., 2018.
[191] Z. Ding, X. Lei, G. K. Karagiannidis, R. Schober, J. Yuan, and V. K. Bhargava, "A survey on non-orthogonal multiple access for 5G networks: Research challenges and future trends," *IEEE J. Sel. Areas Commun.*, vol. 35, no. 10, pp. 2181–2195, Oct. 2017.
[192] M. B. Shahab, R. Abbas, M. Shirvanimoghaddam, and S. J. Johnson, "Grant-free non-orthogonal multiple access for IoT: A survey," *IEEE Commun. Surveys Tuts.*, vol. 22, no. 3, pp. 1805–1838, 3rd Quart., 2020.
[193] C. R. Rao, F. T. Dagefu, G. Verma, P. Spasojevic, and B. M. Sadler, "Scalable sporadic medium access for complex propagation environments," in *Proc. IEEE 29th Annu. Int. Symp. Pers., Indoor Mobile Radio Commun. (PIMRC)*, Sep. 2018, pp. 1–7.
[194] S. Lim, R. L. Rogers, and H. Ling, "A tunable electrically small antenna for ground wave transmission," *IEEE Trans. Antennas Propag.*, vol. 54, no. 2, pp. 417–421, Feb. 2006.

[195] J. Choi, F. T. Dagefu, B. M. Sadler, and K. Sarabandi, "Electrically small folded dipole antenna for HF and low-VHF bands," *IEEE Antennas Wireless Propag. Lett.*, vol. 15, pp. 718–721, 2016.
[196] J. Choi, K. Sarabandi, F. T. Dagefu, and B. M. Sadler, "A non-Foster matched dipole for a low-VHF mobile transmitter system," in *Proc. IEEE Int. Symp. Antennas Propag. USNC/URSI Nat. Radio Sci. Meeting*, Jul. 2017, pp. 2357–2358.
[197] M. Calvo-Fullana, F. T. Dagefu, B. M. Sadler, and A. Ribeiro, "Multi-mode autonomous communication systems," in *Proc. 53rd Asilomar Conf. Signals, Syst., Comput.*, Nov. 2019, pp. 1005–1009.
[198] H. Carrillo, P. Dames, V. Kumar, and J. A. Castellanos, "Autonomous robotic exploration using a utility function based on Rényi's general theory of entropy," *Auto. Robots*, vol. 42, no. 2, pp. 235–256, Feb. 2018.
[199] S. Geirhofer, J. Z. Sun, L. Tong, and B. M. Sadler, "Cognitive frequency hopping based on interference prediction: Theory and experimental results," *ACM SIGMOBILE Mobile Comput. Commun. Rev.*, vol. 13, no. 2, pp. 49–61, Sep. 2009.
[200] J. Zhou, N. Reiskarimian, J. Diakonikolas, T. Dinc, T. Chen, G. Zussman, and H. Krishnaswamy, "Integrated full duplex radios," *IEEE Commun. Mag.*, vol. 55, no. 4, pp. 142–151, Apr. 2017.
[201] M. Adrat, R. Keller, M. Tschauner, S. Wilden, V. Le Nir, T. Riihonen, M. Bowyer, and K. Pärlin, "Full-duplex radio—Increasing the spectral efficiency for military applications," in *Proc. Int. Conf. Mil. Commun. Inf. Syst. (ICMCIS)*, May 2019, pp. 1–5.
[202] K. Pärlin, T. Riihonen, R. Wichman, and D. Korpi, "Transferring the full-duplex radio technology from wireless networking to defense and security," in *Proc. 52nd Asilomar Conf. Signals, Syst., Comput.*, Oct. 2018, pp. 2196–2201.

BRIAN M. SADLER (Life Fellow, IEEE) received the B.S. and M.S. degrees in electrical engineering from the University of Maryland, College Park, MD, USA, and the Ph.D. degree in electrical engineering from the University of Virginia, Charlottesville, VA, USA. He is the U.S. Army Senior Research Scientist for Intelligent Systems and a fellow of the DEVCOM Army Research Laboratory (ARL), Adelphi, MD, USA. His research interests include multi-agent intelligent systems, networking, signal processing, and information science. He received the Best Paper Awards from the IEEE Signal Processing Society, in 2006 and 2010, several ARL and Army Research and Development Awards, and the 2008 Outstanding Invention of the Year Award from the University of Maryland. He also received the Presidential Rank Award, in 2021. He has been a Distinguished Lecturer of the IEEE Signal Processing and IEEE Communications Societies and an Editor of several journals, such as IEEE JOURNAL ON SELECTED AREAS IN COMMUNICATIONS, IEEE TRANSACTIONS ON SIGNAL PROCESSING, and IEEE TRANSACTIONS ON ROBOTICS.

FIKADU T. DAGEFU (Senior Member, IEEE) received the B.S. degree in electrical engineering from the University of Texas at Austin, in 2007, and the M.S. and Ph.D. degrees in electrical engineering from the University of Michigan, Ann Arbor, MI, USA, in 2009 and 2012, respectively. He is currently a Research Scientist with the DEVCOM Army Research Laboratory, Adelphi, MD, USA. His research interests include wireless channel modeling, small antennas, heterogeneous networking, optical communications, and localization. He serves as an Associate Editor for IEEE ANTENNAS AND WIRELESS PROPAGATION LETTERS (AWPL) and *Radio Science Letters* (RSL).

JEFFREY N. TWIGG (Member, IEEE) received the B.S. and M.S. degrees in engineering mechanics from the Virginia Polytechnic Institute and State University, Blacksburg, VA, USA, in 2008 and 2009, respectively, and the Ph.D. degree in mechanical engineering from the University of Maryland, in 2022. Since 2010, he has been a Computer Engineer with the Intelligence for Robotics Branch, DEVCOM Army Research Laboratory. He has authored more than 30 papers on the topics of autonomous communication mapping, distributed beamforming, and robotic parasitic antenna arrays. His research interests include the characterization of radio frequency signals in complex environments with ground robotic agents and multi-robot control for enhancing the reliability and range of wireless communication in the VHF and UHF bands. He served as a Program Committee Member for the 2021 International Conference on Autonomous Systems. He was a recipient of the U.S. Department of the Army Civilian Service Commendation Medal and the Best Paper Award from the 2019 International Conference on Military Communications and Information Systems.

GUNJAN VERMA received the B.S. degree in mathematics, computer science, and economics from Rutgers University, the M.S. degree in biostatistics from Duke University, and the M.S. degree in mathematics from Johns Hopkins University. Since 2009, he has been with the DEVCOM Army Research Laboratory, Adelphi, MD, USA, where he is currently a Computer Scientist. He is the Government Research Lead in the Internet of Battlefield Things Collaborative Research Alliance, a ten-year research endeavor between ARL and seven universities across the nation. He is also one of ARL's primary researchers in collaborative projects at Rice University and UT-Austin studying the use of machine learning to improve tactical wireless networking performance. His work has appeared in prominent conferences and journals in the networking, robotics, and machine-learning fields. Software that he has implemented has been used as part of large-scale network simulation tools, and in embedded systems, software-defined radios, and robots used in several major field experiments with domestic and international partners. His research interests include mathematical and statistical modeling and algorithm development to solve a variety of problems arising in wireless networks. He has earned numerous ARL awards for basic research and research leadership.

PREDRAG SPASOJEVIC (Senior Member, IEEE) received the Diploma degree from the School of Electrical Engineering, University of Sarajevo, in 1990, and the M.S. and Ph.D. degrees in electrical engineering from Texas A&M University, College Station, TX, USA, in 1992 and 1999, respectively. From 2000 to 2001, he was with the WINLAB, Department of Electrical and Computer Engineering, Rutgers University, Piscataway, NJ, USA, as a Lucent Postdoctoral Fellow and a Research Professor. He is currently a Professor with the Department of Electrical and Computer Engineering, Rutgers University. Since 2001 he has been a member of the WINLAB Research Faculty. From 2017 to 2018, he was a Senior Research Fellow with Oak Ridge-associated universities with the Army Research Laboratory, Adelphi, MD, USA. During the Summer of 2023, he was a Visiting Associate Professor with RIEC, Tohoku University, Sendai, Japan. His research interests include communication information theory and signal processing.

RICHARD J. KOZICK (Senior Member, IEEE) received the B.S. degree in electrical engineering from Bucknell University, in 1986, the M.S. degree from Stanford University, in 1988, and the Ph.D. degree in electrical engineering from the University of Pennsylvania, in 1992. From 1986 to 1989 and from 1992 to 1993, he was a member of the Technical Staff with AT&T Bell Laboratories. Since 1993, he has been with Bucknell University, where he is currently a Professor of electrical and computer engineering. His research interests include antenna array system design, signal processing, and medical ultrasound imaging. He received the 2006 Best Paper Award from the IEEE Signal Processing Society and the Presidential Award for Teaching Excellence from Bucknell University, in 1999.

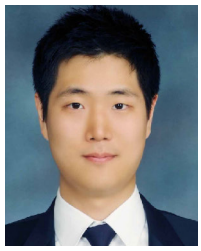

JUSTIN KONG (Senior Member, IEEE) received the B.S. and Ph.D. degrees in electrical engineering from Korea University, Seoul, South Korea, in 2009 and 2015, respectively. In 2010, he visited the University of Southern California, Los Angeles, CA, USA, to conduct collaborative research. In 2015, he was a Postdoctoral Research Professor with Korea University. From 2015 to 2018, he was a Postdoctoral Research Fellow with Nanyang Technological University, Singapore, and he was a Postdoctoral Research Associate with Texas A&M University from 2018 to 2019. In 2019, he joined DEVCOM Army Research Laboratory, where he is currently a Research Scientist. His research interests include information theory, signal processing for wireless communications, and stochastic geometry and its applications in wireless communications. He received the Bronze Prizes in the Samsung Humantech Paper Contest in 2012 and 2013, respectively. He was a recipient of the IEEE TCGCN Best Paper Award from the IEEE ICC 2019.